

Appendix:

Diffusion Language-Shapelets for Semi-supervised Time-Series Classification

Zhen Liu¹, Wenbin Pei^{2,3}, Disen Lan¹, Qianli Ma^{1*}

¹School of Computer Science and Engineering, South China University of Technology, Guangzhou, China

²School of Computer Science and Technology, Dalian University of Technology, Dalian, China

³Key Laboratory of Social Computing and Cognitive Intelligence (Dalian University of Technology), Ministry of Education
cszhenliu@mail.scut.edu.cn, peiwenbin@dlut.edu.cn, 202130480657@mail.scut.edu.cn, qianlima@scut.edu.cn

A Details of Datasets

The UCR time series archive (Dau et al. 2019) is widely utilized in time series classification studies (Ismail Fawaz et al. 2019; Middlehurst, Schäfer, and Bagnall 2023), which collects 128 time series datasets from various real-world scenarios like traffic, medicine, and human actions. Each UCR time series data contains a single training and testing set. However, most UCR time series datasets have a small number of samples in the training set and are even smaller than the test set. Furthermore, the original UCR dataset lacks a dedicated validation set for model training. In such a case, semi-supervised classification is performed directly on the training set of the original UCR dataset, which easily results in obtaining classification test results with a large bias. Following the suggestion given by (Dau et al. 2019; Liu et al. 2023), we initially merged the provided training and test sets for each UCR dataset. Subsequently, following (Liu et al. 2023), we restricted having an average of at least 30 samples per class within each dataset to ensure more stable classification test results. Therefore, we used 106 datasets from the original 128 UCR datasets for experimental analysis, and please refer to Table 1 for specific statistical information. Finally, we used a five-fold cross-validation method to obtain the training-validation-test set for each dataset according to the ratio of 60%-20%-20%. Notably, for UCR time series datasets containing missing values, we employed the mean imputation method for preprocessing.

Regarding the natural language descriptions associated with the 106 UCR time series datasets mentioned in Table 1, we formulated these descriptions by utilizing the original keyword information provided by the respective UCR dataset providers.

B Details of Baselines

In this study, we have chosen baselines that encompass two main aspects: (i) semi-supervised classification methods mainly for time series data; and (ii) shapelet-based time series classification methods. Concerning the existing SSL methods mainly for time series, we have selected 10 baselines as follows:

- Supervised: We solely employ the provided labeled data to train the model for supervised classification, utilizing the cross-entropy loss.
- Pseudo-Label¹: Lee et al. (2013) used soft labels predicted with high confidence by the classifier during training as pseudo-labels for unlabeled data for semi-supervised classification.
- Temporal Ensembling²: Laine and Aila (2016) form a consensus prediction of the unknown labels (or unlabeled data) using the outputs of the network-in-training on different epochs as a regularization strategy for semi-supervised classification.
- LPDeepSSL³: Iscen et al. (2019) employ a transductive label propagation method on the learned embeddings to obtain the pseudo-labels of unlabeled data for semi-supervised classification.
- MTL⁴: Jawed, Grabocka, and Schmidt-Thieme (2020) introduce a forecasting task to exploit the unlabeled time series data. Especially, they established multi-task learning approaches by using forecasting as an auxiliary task for time series semi-supervised classification.
- TS-TCC⁵: Eldele et al. (2021) design an unsupervised temporal and contextual contrastive learning loss for representation learning. Following (Liu et al. 2023), we use TS-TCC as a time series SSL baseline.
- SemiTime⁶: Fan et al. (2021) design a temporal relation prediction loss that operates on segments from labeled and unlabeled time series, specifically on past-future pairs. This mechanism is used to enhance time series semi-supervised classification.
- SSSTC⁷: Xi et al. (2022) design a temporal relation prediction loss based on the split “past-anchor-future” segments from labeled and unlabeled time series, thus contributing to time series semi-supervised classification.

¹https://github.com/iBelieveCJM/pseudo_label-pytorch

²<https://github.com/ferretj/temporal-ensembling>

³<https://github.com/ahmetius/LP-DeepSSL>

⁴<https://github.com/super-shayan/semi-super-ts-clf>

⁵<https://github.com/emadeldeen24/TS-TCC>

⁶<https://github.com/haoyfan/SemiTime>

⁷<https://github.com/mrxiliang/ssstsc>

*Qianli Ma is the corresponding author.

- MTFC ⁸: Wei et al. (2023) propose a time-frequency based multi-task learning method for time series semi-supervised classification. Specially, they use a forecasting task based on MTL for learning time-frequency features from unlabeled data.
- TS-TFC ⁹: Liu et al. (2023) propose a temporal-frequency co-training framework for time series semi-supervised classification. In particular, they employ complementary information from time-domain and frequency-domain views to select high-quality pseudo-labels for unlabeled data learning.

For the shapelet-based time series classification methods, we combined them with the pseudo-labeling strategy in DiffShape for time series semi-supervised classification. The specific information on the above baselines is as follows:

- ST ¹⁰: Lines et al. (2012) incorporate a shapelet transformation method to discover k best shapelets for time series classification.
- LTS ¹¹: Grabocka et al. (2014) first propose learning shapelets perspective based on a classification objective function via stochastic gradient learning for time series classification.
- FSS ¹²: Ji et al. (2019) introduce a fast shapelet selection method from original subsequences for time series classification.
- ADSN ¹³: Ma et al. (2020) propose adversarial dynamic shapelet networks to learn shapelets for time series classification.

For the above four methods, we first train them using labeled data. Then, we use the trained model to transform the training set (labeled and unlabeled data), validation set, and test set into the corresponding set of shapelets. Finally, we use the above set of shapelets to input into the same encoder and classifier as DiffShape for semi-supervised learning. The pseudo-code of our proposed DiffShape model is shown in Algorithm 1. For the reproduction source code of the above baselines and the source code of DiffShape, please refer to our GitHub: <https://github.com/qianlima-lab/DiffShape>.

C Details of Main Results

For specific and detailed test classification results of DiffShape and the 10 SSL baselines on the 106 UCR time series datasets, kindly consult Table 2 (10% labeling ratio), Table 3 (20% labeling ratio), and Table 4 (40% labeling ratio). To facilitate the presentation and reading of the test classification accuracy results, we did not provide standard deviations of test classification accuracy for each baseline in Tables 2, 3 and 4. Also, we have included the critical difference diagram comparing DiffShape with the 10 SSL baselines in Figure 1.

⁸<https://github.com/Chixuan-Wei/SemiSuperTSC>

⁹<https://github.com/qianlima-lab/TS-TFC>

¹⁰https://github.com/mlpotter/Shapelet_Transform/tree/main

¹¹<https://github.com/benibaeumle/Learning-Shapelets>

¹²<https://github.com/benibaeumle/FSS-Algorithm>

¹³<https://github.com/qianlima-lab/ADSN>

D Details of Comparisons with Shapelet-based TSC Methods

For specific test classification results of DiffShape and four shapelet-based time series classification methods for semi-supervised classification on 12 UCR time series datasets, kindly refer to Table 5 (10% labeling ratio), Table 6 (20% labeling ratio), and Table 7 (40% labeling ratio). To enhance the clarity and readability of the results presentation, we have omitted reporting the standard deviation of the test classification results for each baseline in Tables 5, 6 and 7.

E Details of Results on a Few Labeled Time Series

For supervised classification test results of DiffShape and 2 shapelet-based time series classification methods, as well as 6 SSL methods with only a few labeled samples on 12 UCR time series datasets, kindly refer to Table 8 (2 labeled samples per class), Table 9 (5 labeled samples per class), and Table 10 (10 labeled samples per class). To enhance the clarity and readability of the results presentation, we have omitted reporting the standard deviation of the test classification results for each baseline in Tables 8, 9 and 10.

F Details of Ablation Study

For detailed results of the test classification accuracy from the DiffShape ablation experiments on the 12 UCR datasets with a labeling ratio of 10%, please consult Table 11. Additionally, for a comparative analysis of the shapelet visualization achieved by DiffShape and LTS (Grabocka et al. 2014), ADSN (Ma et al. 2020) on the *SonyAIBORobotSurface1* dataset with a labeling ratio of 10%, please refer to Figure 2. Moreover, for t-SNE (Van der Maaten and Hinton 2008) visualization results depicting the embeddings learned by DiffShape, SemiTime (Fan et al. 2021), and TS-TFC (Liu et al. 2023) on the *UWaveGestureLibraryAll* dataset with a labeling ratio of 10%, kindly refer to Figure 3.

G Runtime Analysis

We have chosen the *Trace* dataset (with a total of 200 samples and a sequence length of 275) and the *ChlorineConcentration* dataset (with a total of 4307 samples and a sequence length of 166) for the runtime analysis of various baselines, including seven SSL methods and four shapelet-based methods. To conduct this analysis, we computed the overall runtime for semi-supervised classification using five-fold cross-validation for all baselines, employing a 10% labeling ratio. For consistency, we utilized the same encoder and classifier for semi-supervised classification in each baseline, and all baselines were trained and tested on individual NVIDIA GeForce RTX 3090 GPUs. The runtime statistics for DiffShape and the mentioned baselines are provided in Table 12. Notably, we observed that DiffShape’s runtime is significantly lower compared to MTL (Jawed, Grabocka, and Schmidt-Thieme 2020), SemiTime (Fan et al. 2021), SSSTC (Xi et al. 2022), and MTFC (Wei et al. 2023). Additionally, DiffShape’s runtime is also lower than that of the shapelet-based approaches. Furthermore, our analysis

Algorithm 1: The pseudo-code of DiffShape model.

Input : Convolution layer $w_f(\cdot)$, 1-D U-Net $g(\cdot)$ for diffusion learning, Shapelets transformation encoder $w_s(\cdot)$, Frozen Pre-trained T5 language encoder $z(\cdot)$, Text projection head $h(\cdot)$, Classifier $w_c(\cdot)$, Number of Shapelets k , Length of a shapelet $L = \eta * N$, Sampling steps T , Batch size: B , Number of epochs: E_{max} , Number of iterations: $Iter_{max}$;

```
1 Obtain all real subsequences  $S_{train}$  from the labeled set  $\mathcal{D}^L$  and the unlabeled set  $\mathcal{D}^U$ ;  
2 for  $e \leftarrow 1$  to  $E_{max}$  do  
3   Shuffle training set  $S_{train}$ ;  
4   for  $iter \leftarrow 1$  to  $Iter_{max}$  do  
5     Fetch real subsequences  $S \in \mathbb{R}^{B \times L \times J}$  from shuffled  $S_{train}$ ;  
6     Obtain shapelets  $\mathbf{S}_0 = w_f(S)$ , where  $\mathbf{S}_0 \in \mathbb{R}^{B \times L \times k}$ ;  
7     Search similar real subsequences shapelets  $\mathbf{S}_r$  via  $\mathbf{S}_0$  from  $S$ , where  $\mathbf{S}_r \in \mathbb{R}^{B \times L \times k}$ ;  
8     Obtain shapelets  $\mathbf{S}_t$  via Eq. (2) added injected noise through a forward diffusion process;  
9     Training  $g(\cdot)$  via  $\mathcal{L}_{diff}$  through reverse diffusion process;  
10    Obtain sampling shapelets  $\hat{\mathbf{S}}_0$  via Eq. (8) and Eq. (9) by  $g(\cdot)$  of iteration  $T$  steps using only labeled shapelets;  
11    Obtain shapelets transformation embeddings  $r_s = w_s(\mathbf{S}_0, \hat{\mathbf{S}}_0)$ ;  
12    Obtain pseudo-labels of unlabeled data in  $\mathbf{S}_0$  via the predicted soft labels with high confidence of  $w_c(r_s)$ ;  
13    Construct natural language descriptions  $\mathbf{L}$  using the labels and pseudo-labels within  $\mathbf{S}_0$ ;  
14    Obtain language embeddings  $r_l = h(z(\mathbf{L}))$ ;  
15    Training  $r_s$  and  $r_l$  via  $\mathcal{L}_{lan}$  through contrastive language-shapelets learning;  
16    Update DiffShape ( $w_f(\cdot)$ ,  $g(\cdot)$ ,  $w_s(\cdot)$ ,  $h(\cdot)$  and  $w_c(\cdot)$ ) model via  $\mathcal{L}_{total}$ ;  
17  end  
18 end  
Output:  $w_f(\cdot)$ ,  $g(\cdot)$ ,  $w_s(\cdot)$ ,  $h(\cdot)$  and  $w_c(\cdot)$ .
```

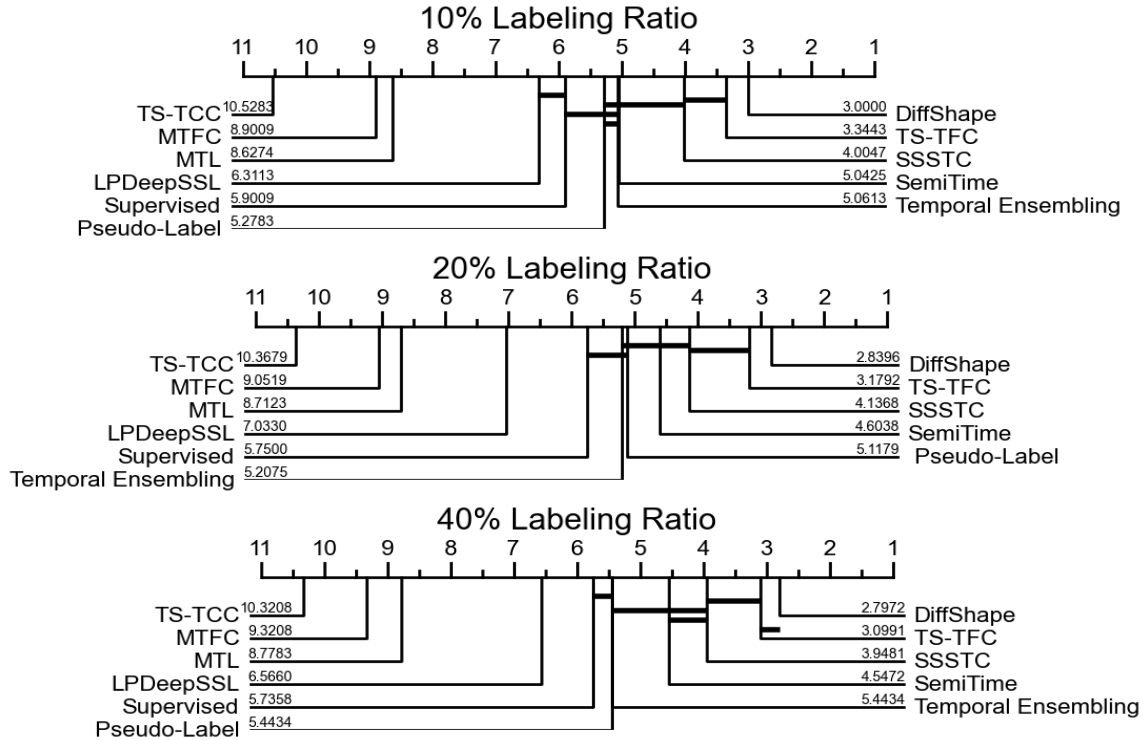


Figure 1: Critical Difference (CD) diagram (Demšar 2006) showing pairwise statistical difference comparison of 11 SSL methods on 106 UCR time series datasets. The CD diagram provides statistical insight into whether the differences are significant. By comparing the CD value of DiffShape with other 11 SSL methods, we find that the classification performance of DiffShape is significant compared to the other 11 methods.

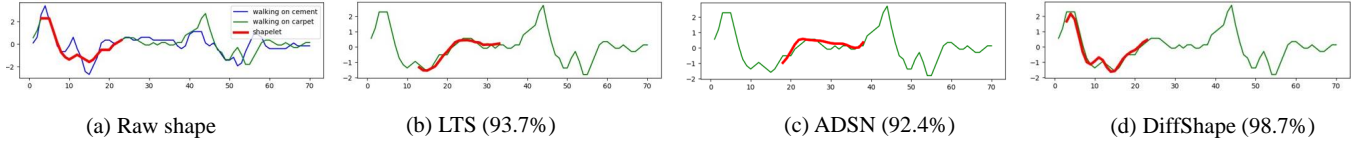


Figure 2: The visualization of shapelet on the *SonyAIBORobotSurface1* dataset with a 10% labeling ratio. The test accuracy is in parentheses. (a) represents a ground truth shapelet of *walking on carpet* class. The position of shapelet learned by (b) LTS and (c) ADSN is away from the ground truth in (a), while the position of shapelet obtained by (d) DiffShape is closer to the ground truth in (a).

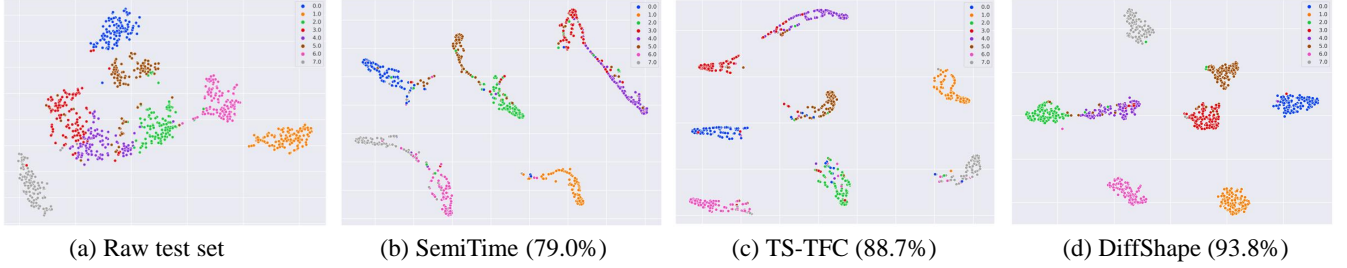


Figure 3: The t-SNE visualization on the *UWaveGestureLibraryAll* dataset with a 10% labeling ratio. The test accuracy is in parentheses. Comparing (a) Raw test set, (b) SemiTime and (c) TS-TFC, we find that the embeddings obtained by DiffShape are more discriminative between classes.

unveiled that Shapelet Transform (ST) (Lines et al. 2012), which is employed for time series classification via the identification of k best shapelets, displays a runtime that positively correlates with the sequence length of the samples. However, this correlation is not significantly observed with the total number of samples. On the contrary, the runtimes of other methods (LTS, ADSN, TS-TFC, and DiffShape) exhibit a positive correlation with the total number of samples.

| ID | Name | # Total numbers | # Classes | # Length | ID | Name | # Total numbers | # Classes | # Length |
|----|------------------------------|-----------------|-----------|----------|-----|--------------------------------|-----------------|-----------|----------|
| 1 | AllGestureWiimoteX | 1000 | 10 | Vary | 54 | Lightning2 | 121 | 2 | 637 |
| 2 | AllGestureWiimoteY | 1000 | 10 | Vary | 55 | Mallat | 2400 | 8 | 1024 |
| 3 | AllGestureWiimoteZ | 1000 | 10 | Vary | 56 | Meat | 120 | 3 | 448 |
| 4 | ArrowHead | 211 | 3 | 251 | 57 | MedicalImages | 1141 | 10 | 99 |
| 5 | BME | 180 | 3 | 128 | 58 | MelbournePedestrian | 3633 | 10 | 24 |
| 6 | Car | 120 | 4 | 577 | 59 | MiddlePhalanxOutlineAgeGroup | 554 | 3 | 80 |
| 7 | CBF | 930 | 3 | 128 | 60 | MiddlePhalanxOutlineCorrect | 891 | 2 | 80 |
| 8 | Chinatown | 363 | 2 | 24 | 61 | MiddlePhalanxTW | 553 | 6 | 80 |
| 9 | ChlorineConcentration | 4307 | 3 | 166 | 62 | MixedShapesRegularTrain | 2925 | 5 | 1024 |
| 10 | CinCECGTorso | 1420 | 4 | 1639 | 63 | MixedShapesSmallTrain | 2525 | 5 | 1024 |
| 11 | Computers | 500 | 2 | 720 | 64 | MoteStrain | 1272 | 2 | 84 |
| 12 | CricketX | 780 | 12 | 300 | 65 | NonInvasiveFetalECGThorax1 | 3765 | 42 | 750 |
| 13 | CricketY | 780 | 12 | 300 | 66 | NonInvasiveFetalECGThorax2 | 3765 | 42 | 750 |
| 14 | CricketZ | 780 | 12 | 300 | 67 | OSULeaf | 442 | 6 | 427 |
| 15 | Crop | 24000 | 24 | 46 | 68 | PhalangesOutlinesCorrect | 2658 | 2 | 80 |
| 16 | DiatomSizeReduction | 322 | 4 | 345 | 69 | Phoneme | 2110 | 39 | 1024 |
| 17 | DistalPhalanxOutlineAgeGroup | 539 | 3 | 80 | 70 | PLAID | 1074 | 11 | Vary |
| 18 | DistalPhalanxOutlineCorrect | 876 | 2 | 80 | 71 | Plane | 210 | 7 | 144 |
| 19 | DistalPhalanxTW | 539 | 6 | 80 | 72 | PowerCons | 360 | 2 | 144 |
| 20 | DodgerLoopGame | 158 | 2 | 288 | 73 | ProximalPhalanxOutlineAgeGroup | 605 | 3 | 80 |
| 21 | DodgerLoopWeekend | 158 | 2 | 288 | 74 | ProximalPhalanxOutlineCorrect | 891 | 2 | 80 |
| 22 | Earthquakes | 461 | 2 | 512 | 75 | ProximalPhalanxTW | 605 | 6 | 80 |
| 23 | ECG200 | 200 | 2 | 96 | 76 | RefrigerationDevices | 750 | 3 | 720 |
| 24 | ECG5000 | 5000 | 5 | 140 | 77 | ScreenType | 750 | 3 | 720 |
| 25 | ECGFiveDays | 884 | 2 | 136 | 78 | SemgHandGenderCh2 | 900 | 2 | 1500 |
| 26 | ElectricDevices | 16637 | 7 | 96 | 79 | SemgHandMovementCh2 | 900 | 6 | 1500 |
| 27 | EOGHorizontalSignal | 724 | 12 | 1250 | 80 | SemgHandSubjectCh2 | 900 | 5 | 1500 |
| 28 | EOGVerticalSignal | 724 | 12 | 1250 | 81 | ShapeletSim | 200 | 2 | 500 |
| 29 | EthanolLevel | 1004 | 4 | 1751 | 82 | SmallKitchenAppliances | 750 | 3 | 720 |
| 30 | FaceAll | 2250 | 14 | 131 | 83 | SmoothSubspace | 300 | 3 | 15 |
| 31 | FacesUCR | 2250 | 14 | 131 | 84 | SonyAIBORobotSurface1 | 621 | 2 | 70 |
| 32 | Fish | 350 | 7 | 463 | 85 | SonyAIBORobotSurface2 | 980 | 2 | 65 |
| 33 | FordA | 4921 | 2 | 500 | 86 | StarLightCurves | 9236 | 3 | 1024 |
| 34 | FordB | 4446 | 2 | 500 | 87 | Strawberry | 983 | 2 | 235 |
| 35 | FreezerRegularTrain | 3000 | 2 | 301 | 88 | SwedishLeaf | 1125 | 15 | 128 |
| 36 | FreezerSmallTrain | 2878 | 2 | 301 | 89 | Symbols | 1020 | 6 | 398 |
| 37 | GesturePebbleZ1 | 304 | 6 | Vary | 90 | SyntheticControl | 600 | 6 | 60 |
| 38 | GesturePebbleZ2 | 304 | 6 | Vary | 91 | ToeSegmentation1 | 268 | 2 | 277 |
| 39 | GunPoint | 200 | 2 | 150 | 92 | ToeSegmentation2 | 166 | 2 | 343 |
| 40 | GunPointAgeSpan | 451 | 2 | 150 | 93 | Trace | 200 | 4 | 275 |
| 41 | GunPointMaleVersusFemale | 451 | 2 | 150 | 94 | TwoLeadECG | 1162 | 2 | 82 |
| 42 | GunPointOldVersusYoung | 451 | 2 | 150 | 95 | TwoPatterns | 5000 | 4 | 128 |
| 43 | Ham | 214 | 2 | 431 | 96 | UMD | 180 | 3 | 150 |
| 44 | HandOutlines | 1370 | 2 | 2709 | 97 | UWaveGestureLibraryAll | 4478 | 8 | 945 |
| 45 | Haptics | 463 | 5 | 1092 | 98 | UWaveGestureLibraryX | 4478 | 8 | 315 |
| 46 | Herring | 128 | 2 | 512 | 99 | UWaveGestureLibraryY | 4478 | 8 | 315 |
| 47 | HouseTwenty | 159 | 2 | 2000 | 100 | UWaveGestureLibraryZ | 4478 | 8 | 315 |
| 48 | InlineSkate | 650 | 7 | 1882 | 101 | Wafer | 7164 | 2 | 152 |
| 49 | InsectEPGRegularTrain | 311 | 3 | 601 | 102 | Wine | 111 | 2 | 234 |
| 50 | InsectEPGSmallTrain | 266 | 3 | 601 | 103 | WordSynonyms | 905 | 25 | 270 |
| 51 | InsectWingbeatSound | 2200 | 11 | 256 | 104 | Worms | 258 | 5 | 900 |
| 52 | ItalyPowerDemand | 1096 | 2 | 24 | 105 | WormsTwoClass | 258 | 2 | 900 |
| 53 | LargeKitchenAppliances | 750 | 3 | 720 | 106 | Yoga | 3300 | 2 | 426 |

Table 1: The detailed information of the 106 UCR time series datasets. “Total numbers” represent the overall count of samples within the time series dataset. “Classes” indicates the number of classes present within each time series dataset. “Length” refers to the sequence length of individual time series within the corresponding dataset. The presence of “Vary” signifies that the dataset includes instances with missing values.

| ID | Dataset | Supervised Pseudo-Label | | TE | LPDeepSSL | MTL | TS-TCC | SemiTime | SSSTC | MTFC | TS-TFC | DiffShape |
|----|------------------------------|-------------------------|--------------|--------------|-----------|-------|--------|--------------|--------------|--------------|--------------|--------------|
| 1 | AllGestureWiimoteX | 0.518 | 0.559 | 0.538 | 0.424 | 0.422 | 0.156 | 0.496 | 0.503 | 0.415 | 0.547 | 0.558 |
| 2 | AllGestureWiimoteY | 0.580 | 0.562 | 0.589 | 0.578 | 0.436 | 0.181 | 0.555 | 0.587 | 0.409 | 0.619 | 0.627 |
| 3 | AllGestureWiimoteZ | 0.537 | 0.537 | 0.540 | 0.375 | 0.346 | 0.209 | 0.503 | 0.541 | 0.227 | 0.543 | 0.552 |
| 4 | ArrowHead | 0.687 | 0.758 | 0.744 | 0.725 | 0.565 | 0.308 | 0.765 | 0.763 | 0.403 | 0.711 | 0.759 |
| 5 | BME | 0.633 | 0.672 | 0.694 | 0.661 | 0.667 | 0.550 | 0.678 | 0.672 | 0.517 | 0.694 | 0.872 |
| 6 | Car | 0.658 | 0.592 | 0.667 | 0.467 | 0.558 | 0.250 | 0.662 | 0.575 | 0.425 | 0.520 | 0.683 |
| 7 | CBF | 0.998 | 0.998 | 0.994 | 0.997 | 0.975 | 0.975 | 0.993 | 0.996 | 0.985 | 0.999 | 1.000 |
| 8 | Chinatown | 0.970 | 0.961 | 0.970 | 0.973 | 0.419 | 0.712 | 0.970 | 0.975 | 0.959 | 0.973 | 0.981 |
| 9 | ChlorineConcentration | 0.604 | 0.722 | 0.733 | 0.737 | 0.607 | 0.537 | 0.719 | 0.682 | 0.575 | 0.744 | 0.749 |
| 10 | CinCECGTorso | 0.911 | 0.940 | 0.925 | 0.927 | 0.881 | 0.702 | 0.915 | 0.934 | 0.613 | 0.998 | 0.982 |
| 11 | Computers | 0.658 | 0.736 | 0.742 | 0.722 | 0.756 | 0.646 | 0.761 | 0.752 | 0.748 | 0.764 | 0.742 |
| 12 | CricketX | 0.535 | 0.535 | 0.515 | 0.505 | 0.492 | 0.126 | 0.524 | 0.599 | 0.389 | 0.590 | 0.608 |
| 13 | CricketY | 0.527 | 0.541 | 0.531 | 0.451 | 0.367 | 0.146 | 0.524 | 0.564 | 0.430 | 0.540 | 0.594 |
| 14 | CricketZ | 0.537 | 0.567 | 0.560 | 0.550 | 0.459 | 0.156 | 0.563 | 0.609 | 0.460 | 0.619 | 0.639 |
| 15 | Crop | 0.674 | 0.667 | 0.667 | 0.656 | 0.624 | 0.410 | 0.628 | 0.685 | 0.595 | 0.685 | 0.701 |
| 16 | DiatomSizeReduction | 0.876 | 0.923 | 0.920 | 0.929 | 0.731 | 0.350 | 0.885 | 0.901 | 0.643 | 0.975 | 0.985 |
| 17 | DistalPhalanxOutlineAgeGroup | 0.822 | 0.821 | 0.824 | 0.820 | 0.764 | 0.753 | 0.790 | 0.776 | 0.764 | 0.826 | 0.838 |
| 18 | DistalPhalanxOutlineCorrect | 0.787 | 0.765 | 0.791 | 0.775 | 0.713 | 0.629 | 0.791 | 0.814 | 0.729 | 0.805 | 0.813 |
| 19 | DistalPhalanxTW | 0.746 | 0.732 | 0.741 | 0.699 | 0.731 | 0.691 | 0.751 | 0.750 | 0.655 | 0.742 | 0.742 |
| 20 | DodgerLoopGame | 0.651 | 0.676 | 0.708 | 0.632 | 0.576 | 0.481 | 0.683 | 0.708 | 0.620 | 0.842 | 0.880 |
| 21 | DodgerLoopWeekend | 0.810 | 0.778 | 0.760 | 0.815 | 0.703 | 0.797 | 0.852 | 0.924 | 0.873 | 0.849 | 0.918 |
| 22 | Earthquakes | 0.795 | 0.775 | 0.796 | 0.825 | 0.595 | 0.602 | 0.741 | 0.785 | 0.829 | 0.790 | 0.803 |
| 23 | ECG200 | 0.946 | 0.942 | 0.941 | 0.936 | 0.939 | 0.896 | 0.942 | 0.790 | 0.785 | 0.950 | 0.875 |
| 24 | ECG5000 | 0.991 | 0.995 | 0.997 | 0.996 | 0.899 | 0.794 | 0.992 | 0.941 | 0.922 | 0.996 | 0.945 |
| 25 | ECGFiveDays | 0.327 | 0.345 | 0.378 | 0.318 | 0.328 | 0.192 | 0.424 | 0.998 | 0.919 | 0.459 | 1.000 |
| 26 | ElectricDevices | 0.318 | 0.318 | 0.313 | 0.337 | 0.293 | 0.166 | 0.379 | 0.395 | 0.265 | 0.443 | 0.799 |
| 27 | EOGHorizontalSignal | 0.798 | 0.792 | 0.798 | 0.798 | 0.798 | 0.798 | 0.770 | 0.854 | 0.720 | 0.801 | 0.820 |
| 28 | EOGVerticalSignal | 0.852 | 0.838 | 0.838 | 0.832 | 0.809 | 0.663 | 0.844 | 0.372 | 0.296 | 0.857 | 0.579 |
| 29 | EthanolLevel | 0.547 | 0.389 | 0.427 | 0.292 | 0.263 | 0.249 | 0.554 | 0.570 | 0.269 | 0.580 | 0.589 |
| 30 | FaceAll | 0.864 | 0.942 | 0.942 | 0.919 | 0.806 | 0.246 | 0.921 | 0.912 | 0.802 | 0.933 | 0.943 |
| 31 | FacesUCR | 0.854 | 0.935 | 0.926 | 0.886 | 0.862 | 0.214 | 0.901 | 0.897 | 0.870 | 0.912 | 0.947 |
| 32 | Fish | 0.829 | 0.589 | 0.569 | 0.389 | 0.446 | 0.143 | 0.757 | 0.734 | 0.334 | 0.354 | 0.777 |
| 33 | FordA | 0.891 | 0.900 | 0.906 | 0.899 | 0.890 | 0.800 | 0.905 | 0.914 | 0.629 | 0.907 | 0.935 |
| 34 | FordB | 0.881 | 0.877 | 0.884 | 0.882 | 0.872 | 0.805 | 0.892 | 0.902 | 0.774 | 0.873 | 0.913 |
| 35 | FreezerRegularTrain | 0.998 | 0.994 | 0.997 | 0.998 | 0.638 | 0.761 | 0.992 | 0.998 | 0.607 | 0.997 | 0.998 |
| 36 | FreezerSmallTrain | 0.999 | 0.998 | 0.999 | 0.998 | 0.848 | 0.760 | 0.997 | 0.998 | 0.618 | 0.999 | 0.999 |
| 37 | GesturePebbleZ1 | 0.651 | 0.586 | 0.593 | 0.563 | 0.591 | 0.187 | 0.677 | 0.714 | 0.622 | 0.434 | 0.671 |
| 38 | GesturePebbleZ2 | 0.622 | 0.691 | 0.671 | 0.538 | 0.577 | 0.208 | 0.629 | 0.708 | 0.655 | 0.460 | 0.783 |
| 39 | GunPoint | 0.735 | 0.955 | 0.945 | 0.910 | 0.765 | 0.545 | 0.957 | 0.890 | 0.640 | 0.910 | 0.930 |
| 40 | GunPointAgeSpan | 0.858 | 0.949 | 0.920 | 0.942 | 0.882 | 0.774 | 0.969 | 0.982 | 0.879 | 0.982 | 0.956 |
| 41 | GunPointMaleVersusFemale | 0.967 | 0.992 | 0.993 | 0.991 | 0.989 | 0.956 | 0.991 | 0.996 | 0.971 | 0.998 | 0.989 |
| 42 | GunPointOldVersusYoung | 0.927 | 0.820 | 0.845 | 0.891 | 0.765 | 0.601 | 0.938 | 0.971 | 0.697 | 0.985 | 0.956 |
| 43 | Ham | 0.603 | 0.575 | 0.622 | 0.593 | 0.547 | 0.481 | 0.654 | 0.678 | 0.687 | 0.636 | 0.720 |
| 44 | HandOutlines | 0.800 | 0.811 | 0.832 | 0.777 | 0.643 | 0.639 | 0.805 | 0.812 | 0.736 | 0.875 | 0.880 |
| 45 | Haptics | 0.382 | 0.344 | 0.363 | 0.305 | 0.290 | 0.203 | 0.319 | 0.372 | 0.283 | 0.370 | 0.415 |
| 46 | Herring | 0.617 | 0.579 | 0.549 | 0.579 | 0.601 | 0.562 | 0.616 | 0.556 | 0.563 | 0.618 | 0.657 |
| 47 | HouseTwenty | 0.905 | 0.899 | 0.931 | 0.872 | 0.899 | 0.578 | 0.932 | 0.963 | 0.969 | 0.928 | 0.928 |
| 48 | InlineSkate | 0.239 | 0.294 | 0.362 | 0.360 | 0.257 | 0.161 | 0.215 | 0.251 | 0.162 | 0.428 | 0.315 |
| 49 | InsectEPGRegularTrain | 0.910 | 0.917 | 0.930 | 0.894 | 0.911 | 0.654 | 0.871 | 0.942 | 0.917 | 0.962 | 0.958 |
| 50 | InsectEPGSmallTrain | 0.922 | 0.888 | 0.888 | 0.888 | 0.853 | 0.631 | 0.884 | 0.922 | 0.861 | 0.944 | 0.899 |
| 51 | InsectWingbeatSound | 0.296 | 0.358 | 0.361 | 0.349 | 0.292 | 0.121 | 0.355 | 0.346 | 0.272 | 0.547 | 0.609 |
| 52 | ItalyPowerDemand | 0.947 | 0.964 | 0.955 | 0.971 | 0.875 | 0.886 | 0.960 | 0.939 | 0.951 | 0.965 | 0.972 |
| 53 | LargeKitchenAppliances | 0.857 | 0.857 | 0.832 | 0.835 | 0.756 | 0.603 | 0.868 | 0.819 | 0.597 | 0.843 | 0.792 |
| 54 | Lightning2 | 0.637 | 0.744 | 0.654 | 0.627 | 0.628 | 0.612 | 0.666 | 0.695 | 0.662 | 0.746 | 0.754 |
| 55 | Mallat | 0.960 | 0.982 | 0.980 | 0.958 | 0.437 | 0.159 | 0.940 | 0.890 | 0.401 | 0.988 | 0.973 |
| 56 | Meat | 0.767 | 0.667 | 0.750 | 0.617 | 0.617 | 0.333 | 0.817 | 0.875 | 0.508 | 0.867 | 0.892 |
| 57 | MedicalImages | 0.619 | 0.674 | 0.653 | 0.639 | 0.562 | 0.521 | 0.608 | 0.640 | 0.536 | 0.637 | 0.637 |
| 58 | MelbournePedestrian | 0.854 | 0.842 | 0.846 | 0.847 | 0.525 | 0.501 | 0.847 | 0.854 | 0.589 | 0.864 | 0.867 |
| 59 | MiddlePhalanxOutlineAgeGroup | 0.753 | 0.744 | 0.737 | 0.728 | 0.608 | 0.582 | 0.725 | 0.758 | 0.708 | 0.731 | 0.756 |
| 60 | MiddlePhalanxOutlineCorrect | 0.772 | 0.764 | 0.744 | 0.741 | 0.654 | 0.622 | 0.764 | 0.789 | 0.682 | 0.817 | 0.818 |
| 61 | MiddlePhalanxTW | 0.595 | 0.590 | 0.585 | 0.579 | 0.528 | 0.551 | 0.586 | 0.593 | 0.570 | 0.579 | 0.590 |

| | | | | | | | | | | | | |
|-----------|--------------------------------|--------------|--------------|--------------|--------------|--------------|----------|--------------|--------------|--------------|--------------|--------------|
| 62 | MixedShapesRegularTrain | 0.927 | 0.935 | 0.927 | 0.923 | 0.772 | 0.453 | 0.940 | 0.943 | 0.466 | 0.959 | 0.945 |
| 63 | MixedShapesSmallTrain | 0.914 | 0.921 | 0.926 | 0.913 | 0.795 | 0.454 | 0.924 | 0.917 | 0.414 | 0.962 | 0.933 |
| 64 | MoteStrain | 0.953 | 0.951 | 0.947 | 0.951 | 0.956 | 0.911 | 0.962 | 0.965 | 0.947 | 0.963 | 0.921 |
| 65 | NonInvasiveFetalECGThorax1 | 0.247 | 0.342 | 0.316 | 0.255 | 0.082 | 0.028 | 0.316 | 0.281 | 0.079 | 0.327 | 0.670 |
| 66 | NonInvasiveFetalECGThorax2 | 0.271 | 0.358 | 0.410 | 0.205 | 0.077 | 0.027 | 0.333 | 0.341 | 0.094 | 0.457 | 0.381 |
| 67 | OSULeaf | 0.862 | 0.766 | 0.808 | 0.815 | 0.769 | 0.347 | 0.849 | 0.885 | 0.571 | 0.899 | 0.719 |
| 68 | PhalangesOutlinesCorrect | 0.328 | 0.304 | 0.342 | 0.339 | 0.282 | 0.191 | 0.335 | 0.329 | 0.257 | 0.332 | 0.244 |
| 69 | Phoneme | 0.778 | 0.781 | 0.779 | 0.781 | 0.708 | 0.639 | 0.806 | 0.804 | 0.702 | 0.799 | 0.796 |
| 70 | PLAID | 0.289 | 0.292 | 0.294 | 0.291 | 0.298 | 0.168 | 0.303 | 0.307 | 0.148 | 0.290 | 0.340 |
| 71 | Plane | 0.852 | 0.886 | 0.886 | 0.886 | 0.781 | 0.248 | 0.892 | 0.905 | 0.471 | 0.817 | 0.886 |
| 72 | PowerCons | 0.811 | 0.822 | 0.828 | 0.764 | 0.786 | 0.778 | 0.832 | 0.789 | 0.814 | 0.811 | 0.903 |
| 73 | ProximalPhalanxOutlineAgeGroup | 0.822 | 0.848 | 0.828 | 0.845 | 0.668 | 0.783 | 0.817 | 0.835 | 0.655 | 0.826 | 0.833 |
| 74 | ProximalPhalanxOutlineCorrect | 0.825 | 0.785 | 0.811 | 0.814 | 0.689 | 0.681 | 0.833 | 0.845 | 0.731 | 0.842 | 0.824 |
| 75 | ProximalPhalanxTW | 0.770 | 0.785 | 0.772 | 0.790 | 0.676 | 0.724 | 0.762 | 0.797 | 0.706 | 0.775 | 0.780 |
| 76 | RefrigerationDevices | 0.563 | 0.489 | 0.512 | 0.533 | 0.551 | 0.547 | 0.487 | 0.475 | 0.567 | 0.567 | 0.507 |
| 77 | ScreenType | 0.532 | 0.551 | 0.581 | 0.545 | 0.552 | 0.395 | 0.505 | 0.575 | 0.573 | 0.521 | 0.563 |
| 78 | SemgHandGenderCh2 | 0.701 | 0.742 | 0.772 | 0.728 | 0.646 | 0.659 | 0.777 | 0.781 | 0.721 | 0.804 | 0.809 |
| 79 | SemgHandMovementCh2 | 0.390 | 0.414 | 0.417 | 0.389 | 0.303 | 0.211 | 0.400 | 0.416 | 0.329 | 0.423 | 0.466 |
| 80 | SemgHandSubjectCh2 | 0.662 | 0.601 | 0.610 | 0.580 | 0.567 | 0.437 | 0.664 | 0.688 | 0.493 | 0.691 | 0.712 |
| 81 | ShapeletSim | 0.970 | 0.965 | 0.960 | 0.995 | 0.730 | 0.500 | 0.820 | 0.880 | 0.885 | 0.995 | 0.950 |
| 82 | SmallKitchenAppliances | 0.724 | 0.744 | 0.743 | 0.741 | 0.707 | 0.593 | 0.733 | 0.759 | 0.723 | 0.740 | 0.700 |
| 83 | SmoothSubspace | 0.840 | 0.827 | 0.843 | 0.873 | 0.637 | 0.543 | 0.870 | 0.893 | 0.679 | 0.897 | 0.877 |
| 84 | SonyAIBORobotSurface1 | 0.990 | 0.994 | 0.992 | 0.994 | 0.973 | 0.971 | 0.992 | 0.989 | 0.968 | 0.994 | 0.987 |
| 85 | SonyAIBORobotSurface2 | 0.986 | 0.989 | 0.984 | 0.984 | 0.971 | 0.964 | 0.989 | 0.994 | 0.932 | 0.991 | 0.985 |
| 86 | StarLightCurves | 0.951 | 0.976 | 0.976 | 0.976 | 0.516 | 0.847 | 0.977 | 0.950 | 0.868 | 0.978 | 0.897 |
| 87 | Strawberry | 0.698 | 0.927 | 0.932 | 0.930 | 0.755 | 0.643 | 0.928 | 0.938 | 0.750 | 0.939 | 0.940 |
| 88 | SwedishLeaf | 0.701 | 0.876 | 0.891 | 0.877 | 0.725 | 0.145 | 0.727 | 0.819 | 0.468 | 0.877 | 0.889 |
| 89 | Symbols | 0.989 | 0.988 | 0.990 | 0.992 | 0.766 | 0.759 | 0.993 | 0.995 | 0.747 | 0.989 | 0.981 |
| 90 | SyntheticControl | 0.955 | 0.950 | 0.942 | 0.930 | 0.947 | 0.917 | 0.965 | 0.982 | 0.948 | 0.980 | 0.995 |
| 91 | ToeSegmentation1 | 0.888 | 0.855 | 0.870 | 0.840 | 0.866 | 0.713 | 0.892 | 0.914 | 0.852 | 0.896 | 0.899 |
| 92 | ToeSegmentation2 | 0.855 | 0.856 | 0.830 | 0.855 | 0.759 | 0.752 | 0.850 | 0.825 | 0.856 | 0.777 | 0.898 |
| 93 | Trace | 0.875 | 0.830 | 0.805 | 0.885 | 0.830 | 0.485 | 0.860 | 0.965 | 0.780 | 0.935 | 1.000 |
| 94 | TwoLeadECG | 1.000 | 1.000 | 1.000 | 1.000 | 1.000 | 0.787 | 1.000 | 1.000 | 0.993 | 1.000 | 1.000 |
| 95 | TwoPatterns | 0.878 | 0.878 | 0.878 | 0.876 | 0.842 | 0.683 | 0.878 | 0.884 | 0.869 | 0.883 | 0.998 |
| 96 | UMD | 0.844 | 0.833 | 0.872 | 0.828 | 0.739 | 0.583 | 0.889 | 0.939 | 0.644 | 0.900 | 0.872 |
| 97 | UWaveGestureLibraryAll | 0.773 | 0.714 | 0.714 | 0.690 | 0.694 | 0.233 | 0.788 | 0.783 | 0.398 | 0.892 | 0.940 |
| 98 | UWaveGestureLibraryX | 0.727 | 0.728 | 0.723 | 0.710 | 0.552 | 0.310 | 0.733 | 0.746 | 0.388 | 0.757 | 0.793 |
| 99 | UWaveGestureLibraryY | 0.602 | 0.625 | 0.623 | 0.596 | 0.515 | 0.312 | 0.606 | 0.624 | 0.323 | 0.647 | 0.686 |
| 100 | UWaveGestureLibraryZ | 0.692 | 0.690 | 0.684 | 0.677 | 0.569 | 0.299 | 0.673 | 0.693 | 0.399 | 0.700 | 0.722 |
| 101 | Wafer | 0.977 | 0.933 | 0.952 | 0.972 | 0.909 | 0.894 | 0.913 | 0.913 | 0.894 | 0.998 | 0.996 |
| 102 | Wine | 0.583 | 0.576 | 0.540 | 0.667 | 0.578 | 0.504 | 0.667 | 0.738 | 0.487 | 0.583 | 0.676 |
| 103 | WordSynonyms | 0.348 | 0.319 | 0.296 | 0.274 | 0.306 | 0.214 | 0.371 | 0.364 | 0.243 | 0.372 | 0.539 |
| 104 | Worms | 0.550 | 0.535 | 0.570 | 0.504 | 0.523 | 0.437 | 0.579 | 0.542 | 0.446 | 0.574 | 0.549 |
| 105 | WormsTwoClass | 0.658 | 0.737 | 0.710 | 0.694 | 0.667 | 0.547 | 0.740 | 0.710 | 0.524 | 0.686 | 0.717 |
| 106 | Yoga | 0.848 | 0.856 | 0.859 | 0.839 | 0.701 | 0.529 | 0.880 | 0.851 | 0.587 | 0.899 | 0.830 |
| Avg. Rank | | 5.79 | 5.15 | 4.93 | 6.17 | 8.55 | 10.50 | 4.99 | 3.94 | 8.89 | 3.23 | 2.92 |
| Win | | 4 | 5 | 6 | 3 | 1 | 0 | 8 | 17 | 3 | 24 | 51 |
| P-value | | 2.87E-07 | 1.24E-06 | 5.35E-06 | 5.66E-08 | 5.43E-19 | 1.88E-26 | 3.84E-06 | 1.63E-05 | 1.02E-21 | 4.08E-03 | - |

Table 2: The detailed test classification accuracy comparisons on 106 UCR time series datasets with a 10% labeling ratio. Win denotes the number of datasets in which the corresponding baseline achieved the best test accuracy. The best is in **bold**.

| ID | Dataset | Supervised Pseudo-Label | | TE | LPDeepSSL | MTL | TS-TCC | SemiTime | SSSTC | MTFC | TS-TFC | DiffShape |
|----|------------------------------|-------------------------|--------------|--------------|--------------|-------|--------|--------------|--------------|--------------|--------------|--------------|
| 1 | AllGestureWiimoteX | 0.597 | 0.534 | 0.540 | 0.369 | 0.530 | 0.191 | 0.622 | 0.630 | 0.474 | 0.606 | 0.639 |
| 2 | AllGestureWiimoteY | 0.654 | 0.661 | 0.656 | 0.563 | 0.534 | 0.287 | 0.686 | 0.692 | 0.457 | 0.702 | 0.711 |
| 3 | AllGestureWiimoteZ | 0.608 | 0.534 | 0.575 | 0.504 | 0.346 | 0.250 | 0.633 | 0.638 | 0.129 | 0.649 | 0.672 |
| 4 | ArrowHead | 0.825 | 0.810 | 0.805 | 0.796 | 0.797 | 0.451 | 0.881 | 0.858 | 0.455 | 0.910 | 0.893 |
| 5 | BME | 0.683 | 0.794 | 0.739 | 0.722 | 0.633 | 0.556 | 0.728 | 0.706 | 0.556 | 0.806 | 0.978 |
| 6 | Car | 0.775 | 0.692 | 0.750 | 0.542 | 0.458 | 0.258 | 0.775 | 0.769 | 0.333 | 0.767 | 0.792 |
| 7 | CBF | 0.999 | 0.999 | 0.999 | 0.998 | 0.987 | 0.979 | 0.996 | 1.000 | 1.000 | 0.999 | 1.000 |
| 8 | Chinatown | 0.978 | 0.975 | 0.973 | 0.953 | 0.288 | 0.858 | 0.962 | 0.975 | 0.975 | 0.986 | 0.989 |
| 9 | ChlorineConcentration | 0.858 | 0.875 | 0.871 | 0.874 | 0.662 | 0.550 | 0.882 | 0.841 | 0.618 | 0.892 | 0.898 |
| 10 | CinCECGTorso | 0.976 | 0.988 | 0.985 | 0.955 | 0.854 | 0.675 | 0.989 | 0.971 | 0.655 | 1.000 | 0.997 |
| 11 | Computers | 0.794 | 0.830 | 0.792 | 0.776 | 0.798 | 0.650 | 0.802 | 0.816 | 0.808 | 0.796 | 0.796 |
| 12 | CricketX | 0.685 | 0.701 | 0.696 | 0.686 | 0.609 | 0.249 | 0.671 | 0.709 | 0.528 | 0.709 | 0.713 |
| 13 | CricketY | 0.635 | 0.683 | 0.687 | 0.654 | 0.541 | 0.191 | 0.667 | 0.694 | 0.481 | 0.714 | 0.719 |
| 14 | CricketZ | 0.639 | 0.691 | 0.672 | 0.671 | 0.581 | 0.185 | 0.621 | 0.713 | 0.545 | 0.700 | 0.701 |
| 15 | Crop | 0.716 | 0.710 | 0.716 | 0.711 | 0.664 | 0.462 | 0.716 | 0.728 | 0.566 | 0.726 | 0.746 |
| 16 | DiatomSizeReduction | 0.950 | 0.942 | 0.938 | 0.953 | 0.695 | 0.411 | 0.898 | 0.975 | 0.605 | 0.991 | 0.991 |
| 17 | DistalPhalanxOutlineAgeGroup | 0.827 | 0.818 | 0.831 | 0.831 | 0.764 | 0.772 | 0.818 | 0.815 | 0.666 | 0.800 | 0.813 |
| 18 | DistalPhalanxOutlineCorrect | 0.821 | 0.791 | 0.809 | 0.750 | 0.727 | 0.615 | 0.819 | 0.821 | 0.745 | 0.833 | 0.838 |
| 19 | DistalPhalanxTW | 0.777 | 0.754 | 0.787 | 0.767 | 0.733 | 0.698 | 0.753 | 0.800 | 0.605 | 0.774 | 0.765 |
| 20 | DodgerLoopGame | 0.723 | 0.793 | 0.820 | 0.765 | 0.581 | 0.519 | 0.786 | 0.741 | 0.634 | 0.863 | 0.924 |
| 21 | DodgerLoopWeekend | 0.937 | 0.943 | 0.906 | 0.912 | 0.673 | 0.759 | 0.881 | 0.912 | 0.874 | 0.949 | 0.987 |
| 22 | Earthquakes | 0.785 | 0.816 | 0.836 | 0.760 | 0.680 | 0.670 | 0.806 | 0.785 | 0.827 | 0.845 | 0.835 |
| 23 | ECG200 | 0.947 | 0.944 | 0.943 | 0.940 | 0.942 | 0.899 | 0.952 | 0.820 | 0.800 | 0.946 | 0.907 |
| 24 | ECG5000 | 0.999 | 0.997 | 0.998 | 0.993 | 0.983 | 0.840 | 0.998 | 0.947 | 0.930 | 1.000 | 0.969 |
| 25 | ECGFiveDays | 0.550 | 0.557 | 0.547 | 0.454 | 0.460 | 0.213 | 0.572 | 0.999 | 0.946 | 0.584 | 1.000 |
| 26 | ElectricDevices | 0.439 | 0.414 | 0.424 | 0.363 | 0.399 | 0.174 | 0.435 | 0.477 | 0.283 | 0.559 | 0.832 |
| 27 | EOGHorizontalSignal | 0.790 | 0.790 | 0.796 | 0.805 | 0.794 | 0.798 | 0.807 | 0.869 | 0.762 | 0.817 | 0.847 |
| 28 | EOGVerticalSignal | 0.860 | 0.863 | 0.862 | 0.858 | 0.836 | 0.769 | 0.862 | 0.463 | 0.324 | 0.865 | 0.596 |
| 29 | EthanolLevel | 0.663 | 0.636 | 0.625 | 0.539 | 0.244 | 0.253 | 0.640 | 0.611 | 0.254 | 0.686 | 0.689 |
| 30 | FaceAll | 0.952 | 0.966 | 0.963 | 0.937 | 0.856 | 0.425 | 0.958 | 0.967 | 0.893 | 0.972 | 0.982 |
| 31 | FacesUCR | 0.940 | 0.963 | 0.961 | 0.931 | 0.918 | 0.376 | 0.950 | 0.964 | 0.903 | 0.968 | 0.981 |
| 32 | Fish | 0.820 | 0.831 | 0.849 | 0.583 | 0.471 | 0.143 | 0.789 | 0.840 | 0.269 | 0.906 | 0.876 |
| 33 | FordA | 0.909 | 0.912 | 0.913 | 0.907 | 0.907 | 0.866 | 0.931 | 0.923 | 0.774 | 0.914 | 0.941 |
| 34 | FordB | 0.890 | 0.895 | 0.891 | 0.893 | 0.883 | 0.829 | 0.892 | 0.906 | 0.760 | 0.896 | 0.917 |
| 35 | FreezerRegularTrain | 0.997 | 0.997 | 0.997 | 0.898 | 0.681 | 0.758 | 0.995 | 0.998 | 0.820 | 0.998 | 0.999 |
| 36 | FreezerSmallTrain | 0.999 | 0.999 | 0.998 | 0.999 | 0.719 | 0.759 | 0.999 | 0.997 | 0.715 | 0.999 | 1.000 |
| 37 | GesturePebbleZ1 | 0.829 | 0.751 | 0.760 | 0.711 | 0.760 | 0.250 | 0.793 | 0.849 | 0.793 | 0.796 | 0.905 |
| 38 | GesturePebbleZ2 | 0.799 | 0.858 | 0.827 | 0.740 | 0.713 | 0.309 | 0.810 | 0.846 | 0.816 | 0.826 | 0.928 |
| 39 | GunPoint | 0.985 | 0.820 | 0.985 | 0.940 | 0.660 | 0.630 | 0.985 | 0.980 | 0.800 | 0.990 | 0.992 |
| 40 | GunPointAgeSpan | 0.987 | 0.991 | 0.978 | 0.989 | 0.767 | 0.857 | 0.996 | 0.991 | 0.872 | 0.987 | 0.988 |
| 41 | GunPointMaleVersusFemale | 0.987 | 0.993 | 0.991 | 0.892 | 0.993 | 0.982 | 0.996 | 1.000 | 0.682 | 0.998 | 0.999 |
| 42 | GunPointOldVersusYoung | 0.968 | 0.985 | 0.978 | 0.894 | 0.902 | 0.650 | 0.973 | 0.980 | 0.643 | 0.985 | 0.983 |
| 43 | Ham | 0.622 | 0.691 | 0.620 | 0.690 | 0.695 | 0.625 | 0.628 | 0.678 | 0.636 | 0.682 | 0.781 |
| 44 | HandOutlines | 0.868 | 0.868 | 0.848 | 0.834 | 0.682 | 0.639 | 0.833 | 0.843 | 0.708 | 0.897 | 0.900 |
| 45 | Haptics | 0.456 | 0.359 | 0.354 | 0.334 | 0.302 | 0.210 | 0.411 | 0.411 | 0.354 | 0.465 | 0.480 |
| 46 | Herring | 0.617 | 0.610 | 0.579 | 0.580 | 0.610 | 0.602 | 0.587 | 0.626 | 0.562 | 0.601 | 0.687 |
| 47 | HouseTwenty | 0.944 | 0.962 | 0.975 | 0.943 | 0.962 | 0.906 | 0.975 | 0.962 | 0.975 | 0.924 | 0.939 |
| 48 | InlineSkate | 0.366 | 0.412 | 0.408 | 0.441 | 0.299 | 0.163 | 0.346 | 0.369 | 0.277 | 0.528 | 0.395 |
| 49 | InsectEPGRegularTrain | 0.936 | 0.961 | 0.961 | 0.923 | 0.939 | 0.870 | 0.952 | 0.971 | 0.968 | 0.962 | 0.968 |
| 50 | InsectEPGSmallTrain | 0.959 | 0.981 | 0.981 | 0.785 | 0.970 | 0.830 | 0.989 | 0.981 | 0.936 | 0.963 | 0.949 |
| 51 | InsectWingbeatSound | 0.446 | 0.431 | 0.441 | 0.388 | 0.339 | 0.149 | 0.465 | 0.415 | 0.294 | 0.645 | 0.661 |
| 52 | ItalyPowerDemand | 0.961 | 0.967 | 0.964 | 0.973 | 0.830 | 0.929 | 0.962 | 0.964 | 0.908 | 0.970 | 0.975 |
| 53 | LargeKitchenAppliances | 0.912 | 0.915 | 0.901 | 0.883 | 0.892 | 0.620 | 0.883 | 0.923 | 0.615 | 0.913 | 0.897 |
| 54 | Lightning2 | 0.612 | 0.669 | 0.678 | 0.686 | 0.627 | 0.636 | 0.712 | 0.629 | 0.645 | 0.712 | 0.786 |
| 55 | Mallat | 0.987 | 0.988 | 0.990 | 0.816 | 0.545 | 0.263 | 0.990 | 0.988 | 0.546 | 0.991 | 0.980 |
| 56 | Meat | 0.900 | 0.925 | 0.933 | 0.900 | 0.575 | 0.333 | 0.933 | 0.867 | 0.408 | 0.967 | 0.969 |
| 57 | MedicalImages | 0.664 | 0.708 | 0.708 | 0.704 | 0.557 | 0.521 | 0.615 | 0.692 | 0.563 | 0.696 | 0.701 |
| 58 | MelbournePedestrian | 0.893 | 0.869 | 0.872 | 0.869 | 0.664 | 0.629 | 0.893 | 0.900 | 0.577 | 0.899 | 0.902 |
| 59 | MiddlePhalanxOutlineAgeGroup | 0.756 | 0.757 | 0.762 | 0.751 | 0.497 | 0.724 | 0.734 | 0.746 | 0.592 | 0.764 | 0.766 |
| 60 | MiddlePhalanxOutlineCorrect | 0.797 | 0.759 | 0.774 | 0.773 | 0.660 | 0.622 | 0.802 | 0.800 | 0.660 | 0.821 | 0.829 |
| 61 | MiddlePhalanxTW | 0.591 | 0.612 | 0.622 | 0.612 | 0.420 | 0.540 | 0.613 | 0.598 | 0.539 | 0.629 | 0.635 |

| | | | | | | | | | | | | |
|----------|--------------------------------|--------------|--------------|--------------|--------------|--------------|----------|--------------|--------------|----------|--------------|--------------|
| 62 | MixedShapesRegularTrain | 0.958 | 0.945 | 0.952 | 0.944 | 0.812 | 0.561 | 0.961 | 0.961 | 0.557 | 0.972 | 0.967 |
| 63 | MixedShapesSmallTrain | 0.949 | 0.947 | 0.953 | 0.942 | 0.716 | 0.583 | 0.960 | 0.955 | 0.521 | 0.972 | 0.959 |
| 64 | MoteStrain | 0.963 | 0.965 | 0.958 | 0.954 | 0.962 | 0.921 | 0.966 | 0.976 | 0.972 | 0.971 | 0.959 |
| 65 | NonInvasiveFetalECGThorax1 | 0.460 | 0.426 | 0.454 | 0.382 | 0.084 | 0.033 | 0.523 | 0.448 | 0.118 | 0.386 | 0.802 |
| 66 | NonInvasiveFetalECGThorax2 | 0.490 | 0.460 | 0.452 | 0.090 | 0.120 | 0.036 | 0.503 | 0.526 | 0.134 | 0.515 | 0.847 |
| 67 | OSULeaf | 0.930 | 0.923 | 0.928 | 0.886 | 0.840 | 0.410 | 0.942 | 0.937 | 0.516 | 0.935 | 0.858 |
| 68 | PhalangesOutlinesCorrect | 0.337 | 0.339 | 0.379 | 0.308 | 0.295 | 0.192 | 0.388 | 0.346 | 0.180 | 0.338 | 0.348 |
| 69 | Phoneme | 0.821 | 0.823 | 0.817 | 0.806 | 0.694 | 0.632 | 0.827 | 0.836 | 0.677 | 0.838 | 0.829 |
| 70 | PLAID | 0.357 | 0.337 | 0.347 | 0.312 | 0.365 | 0.194 | 0.342 | 0.382 | 0.288 | 0.317 | 0.378 |
| 71 | Plane | 1.000 | 1.000 | 1.000 | 1.000 | 0.929 | 0.486 | 1.000 | 1.000 | 0.405 | 1.000 | 0.986 |
| 72 | PowerCons | 0.814 | 0.844 | 0.831 | 0.822 | 0.786 | 0.761 | 0.851 | 0.856 | 0.814 | 0.814 | 0.903 |
| 73 | ProximalPhalanxOutlineAgeGroup | 0.825 | 0.840 | 0.831 | 0.848 | 0.783 | 0.783 | 0.850 | 0.858 | 0.461 | 0.856 | 0.859 |
| 74 | ProximalPhalanxOutlineCorrect | 0.861 | 0.850 | 0.864 | 0.870 | 0.469 | 0.703 | 0.871 | 0.865 | 0.744 | 0.859 | 0.834 |
| 75 | ProximalPhalanxTW | 0.769 | 0.789 | 0.789 | 0.786 | 0.693 | 0.727 | 0.790 | 0.787 | 0.450 | 0.793 | 0.807 |
| 76 | RefrigerationDevices | 0.576 | 0.639 | 0.627 | 0.572 | 0.583 | 0.564 | 0.596 | 0.543 | 0.565 | 0.655 | 0.576 |
| 77 | ScreenType | 0.601 | 0.648 | 0.656 | 0.640 | 0.601 | 0.409 | 0.591 | 0.629 | 0.551 | 0.639 | 0.619 |
| 78 | SemgHandGenderCh2 | 0.856 | 0.788 | 0.804 | 0.793 | 0.724 | 0.662 | 0.836 | 0.828 | 0.822 | 0.879 | 0.862 |
| 79 | SemgHandMovementCh2 | 0.501 | 0.449 | 0.493 | 0.431 | 0.331 | 0.258 | 0.477 | 0.524 | 0.439 | 0.516 | 0.522 |
| 80 | SemgHandSubjectCh2 | 0.759 | 0.651 | 0.711 | 0.673 | 0.590 | 0.464 | 0.778 | 0.764 | 0.622 | 0.796 | 0.808 |
| 81 | ShapeletSim | 0.970 | 1.000 | 0.995 | 0.995 | 0.735 | 0.695 | 0.975 | 0.970 | 0.965 | 1.000 | 0.971 |
| 82 | SmallKitchenAppliances | 0.759 | 0.764 | 0.781 | 0.763 | 0.739 | 0.585 | 0.747 | 0.765 | 0.771 | 0.797 | 0.741 |
| 83 | SmoothSubspace | 0.893 | 0.927 | 0.903 | 0.933 | 0.790 | 0.867 | 0.937 | 0.897 | 0.792 | 0.883 | 0.888 |
| 84 | SonyAIBORobotSurface1 | 0.997 | 0.990 | 0.989 | 0.990 | 0.990 | 0.974 | 0.992 | 0.997 | 0.987 | 0.997 | 0.991 |
| 85 | SonyAIBORobotSurface2 | 0.990 | 0.995 | 0.996 | 0.987 | 0.981 | 0.979 | 0.989 | 0.994 | 0.985 | 0.996 | 0.992 |
| 86 | StarLightCurves | 0.977 | 0.978 | 0.977 | 0.837 | 0.613 | 0.849 | 0.979 | 0.980 | 0.898 | 0.980 | 0.924 |
| 87 | Strawberry | 0.894 | 0.947 | 0.952 | 0.942 | 0.646 | 0.643 | 0.949 | 0.958 | 0.666 | 0.949 | 0.960 |
| 88 | SwedishLeaf | 0.765 | 0.942 | 0.932 | 0.907 | 0.703 | 0.203 | 0.836 | 0.892 | 0.468 | 0.954 | 0.903 |
| 89 | Symbols | 0.994 | 0.991 | 0.989 | 0.990 | 0.835 | 0.896 | 0.991 | 0.996 | 0.669 | 0.996 | 0.991 |
| 90 | SyntheticControl | 0.985 | 0.988 | 0.985 | 0.983 | 0.978 | 0.885 | 0.988 | 0.982 | 0.965 | 0.995 | 0.995 |
| 91 | ToeSegmentation1 | 0.953 | 0.955 | 0.963 | 0.952 | 0.955 | 0.899 | 0.963 | 0.974 | 0.930 | 0.963 | 0.957 |
| 92 | ToeSegmentation2 | 0.795 | 0.886 | 0.880 | 0.848 | 0.807 | 0.789 | 0.875 | 0.934 | 0.843 | 0.530 | 0.934 |
| 93 | Trace | 0.995 | 0.995 | 0.995 | 0.990 | 0.975 | 0.590 | 1.000 | 1.000 | 0.955 | 1.000 | 1.000 |
| 94 | TwoLeadECG | 1.000 | 1.000 | 1.000 | 1.000 | 1.000 | 0.898 | 1.000 | 1.000 | 0.872 | 1.000 | 1.000 |
| 95 | TwoPatterns | 0.890 | 0.876 | 0.878 | 0.876 | 0.868 | 0.795 | 0.892 | 0.907 | 0.886 | 0.899 | 0.999 |
| 96 | UMD | 0.883 | 0.917 | 0.944 | 0.872 | 0.900 | 0.783 | 0.956 | 0.817 | 0.811 | 0.983 | 0.950 |
| 97 | UWaveGestureLibraryAll | 0.832 | 0.814 | 0.803 | 0.748 | 0.653 | 0.313 | 0.844 | 0.821 | 0.446 | 0.935 | 0.958 |
| 98 | UWaveGestureLibraryX | 0.768 | 0.743 | 0.737 | 0.730 | 0.520 | 0.446 | 0.761 | 0.779 | 0.619 | 0.779 | 0.827 |
| 99 | UWaveGestureLibraryY | 0.664 | 0.654 | 0.659 | 0.650 | 0.523 | 0.420 | 0.666 | 0.670 | 0.536 | 0.680 | 0.747 |
| 100 | UWaveGestureLibraryZ | 0.732 | 0.720 | 0.723 | 0.705 | 0.615 | 0.433 | 0.720 | 0.739 | 0.511 | 0.727 | 0.766 |
| 101 | Wafer | 0.998 | 0.914 | 0.997 | 0.996 | 0.913 | 0.894 | 0.998 | 0.999 | 0.894 | 1.000 | 1.000 |
| 102 | Wine | 0.738 | 0.673 | 0.699 | 0.638 | 0.450 | 0.487 | 0.749 | 0.666 | 0.541 | 0.738 | 0.865 |
| 103 | WordSynonyms | 0.411 | 0.393 | 0.400 | 0.366 | 0.350 | 0.230 | 0.456 | 0.432 | 0.242 | 0.448 | 0.617 |
| 104 | Worms | 0.531 | 0.512 | 0.492 | 0.567 | 0.602 | 0.481 | 0.575 | 0.566 | 0.492 | 0.469 | 0.568 |
| 105 | WormsTwoClass | 0.671 | 0.683 | 0.667 | 0.647 | 0.768 | 0.566 | 0.702 | 0.733 | 0.562 | 0.732 | 0.735 |
| 106 | Yoga | 0.888 | 0.901 | 0.899 | 0.893 | 0.763 | 0.562 | 0.910 | 0.892 | 0.661 | 0.927 | 0.899 |
| Avg Rank | | 5.56 | 4.93 | 5.06 | 6.94 | 8.64 | 10.36 | 4.46 | 3.99 | 9.01 | 3.02 | 2.76 |
| Win | | 3 | 6 | 6 | 3 | 3 | 0 | 10 | 17 | 2 | 27 | 58 |
| P-value | | 2.01E-07 | 9.39E-07 | 3.45E-06 | 3.05E-09 | 4.79E-18 | 1.12E-24 | 3.44E-06 | 8.85E-07 | 1.81E-22 | 3.12E-03 | - |

Table 3: The detailed test classification accuracy comparisons on 106 UCR time series datasets with a 20% labeling ratio. Win denotes the number of datasets in which the corresponding baseline achieved the best test accuracy. The best is in **bold**.

| ID | Dataset | Supervised Pseudo-Label | | TE | LPDeepSSL | MTL | TS-TCC | SemiTime | SSSTC | MTFC | TS-TFC | DiffShape |
|----|------------------------------|-------------------------|--------------|--------------|--------------|--------------|--------|--------------|--------------|--------------|--------------|--------------|
| 1 | AllGestureWiimoteX | 0.676 | 0.674 | 0.702 | 0.557 | 0.556 | 0.195 | 0.670 | 0.653 | 0.514 | 0.685 | 0.760 |
| 2 | AllGestureWiimoteY | 0.766 | 0.677 | 0.743 | 0.685 | 0.587 | 0.272 | 0.763 | 0.787 | 0.468 | 0.786 | 0.805 |
| 3 | AllGestureWiimoteZ | 0.725 | 0.666 | 0.696 | 0.605 | 0.376 | 0.323 | 0.673 | 0.641 | 0.220 | 0.708 | 0.766 |
| 4 | ArrowHead | 0.886 | 0.891 | 0.853 | 0.867 | 0.801 | 0.589 | 0.896 | 0.929 | 0.503 | 0.914 | 0.943 |
| 5 | BME | 0.867 | 0.867 | 0.889 | 0.894 | 0.817 | 0.567 | 0.917 | 0.917 | 0.644 | 0.972 | 0.994 |
| 6 | Car | 0.817 | 0.815 | 0.833 | 0.783 | 0.633 | 0.250 | 0.758 | 0.894 | 0.483 | 0.892 | 0.897 |
| 7 | CBF | 1.000 | 1.000 | 0.999 | 0.999 | 0.984 | 0.985 | 0.999 | 1.000 | 1.000 | 1.000 | 1.000 |
| 8 | Chinatown | 0.984 | 0.986 | 0.982 | 0.986 | 0.288 | 0.910 | 0.982 | 0.989 | 0.987 | 0.986 | 0.992 |
| 9 | ChlorineConcentration | 0.961 | 0.972 | 0.975 | 0.962 | 0.658 | 0.555 | 0.964 | 0.949 | 0.703 | 0.976 | 0.978 |
| 10 | CinCECGTorso | 0.994 | 0.998 | 0.996 | 0.992 | 0.890 | 0.755 | 0.997 | 0.982 | 0.747 | 1.000 | 1.000 |
| 11 | Computers | 0.876 | 0.856 | 0.860 | 0.860 | 0.846 | 0.656 | 0.888 | 0.879 | 0.880 | 0.874 | 0.816 |
| 12 | CricketX | 0.819 | 0.813 | 0.814 | 0.780 | 0.722 | 0.301 | 0.790 | 0.810 | 0.514 | 0.824 | 0.828 |
| 13 | CricketY | 0.729 | 0.790 | 0.765 | 0.787 | 0.715 | 0.203 | 0.791 | 0.767 | 0.531 | 0.808 | 0.819 |
| 14 | CricketZ | 0.789 | 0.815 | 0.804 | 0.808 | 0.674 | 0.228 | 0.797 | 0.809 | 0.663 | 0.833 | 0.839 |
| 15 | Crop | 0.780 | 0.766 | 0.766 | 0.764 | 0.725 | 0.554 | 0.778 | 0.785 | 0.709 | 0.771 | 0.803 |
| 16 | DiatomSizeReduction | 0.994 | 0.978 | 0.967 | 0.988 | 0.833 | 0.351 | 0.957 | 0.998 | 0.456 | 0.997 | 0.999 |
| 17 | DistalPhalanxOutlineAgeGroup | 0.811 | 0.813 | 0.837 | 0.824 | 0.774 | 0.751 | 0.827 | 0.822 | 0.699 | 0.848 | 0.850 |
| 18 | DistalPhalanxOutlineCorrect | 0.822 | 0.837 | 0.832 | 0.816 | 0.708 | 0.615 | 0.842 | 0.838 | 0.743 | 0.834 | 0.845 |
| 19 | DistalPhalanxTW | 0.752 | 0.766 | 0.794 | 0.763 | 0.708 | 0.698 | 0.794 | 0.764 | 0.687 | 0.805 | 0.810 |
| 20 | DodgerLoopGame | 0.861 | 0.869 | 0.850 | 0.862 | 0.612 | 0.481 | 0.818 | 0.855 | 0.677 | 0.899 | 0.949 |
| 21 | DodgerLoopWeekend | 0.930 | 0.956 | 0.924 | 0.968 | 0.748 | 0.854 | 0.962 | 0.950 | 0.949 | 0.975 | 0.994 |
| 22 | Earthquakes | 0.885 | 0.891 | 0.890 | 0.910 | 0.773 | 0.670 | 0.915 | 0.807 | 0.859 | 0.885 | 0.866 |
| 23 | ECG200 | 0.932 | 0.955 | 0.953 | 0.952 | 0.947 | 0.910 | 0.950 | 0.945 | 0.770 | 0.957 | 0.916 |
| 24 | ECG5000 | 1.000 | 0.999 | 0.999 | 0.999 | 0.987 | 0.847 | 1.000 | 0.958 | 0.948 | 1.000 | 0.976 |
| 25 | ECGFiveDays | 0.645 | 0.631 | 0.633 | 0.577 | 0.603 | 0.231 | 0.650 | 1.000 | 0.865 | 0.724 | 1.000 |
| 26 | ElectricDevices | 0.577 | 0.563 | 0.510 | 0.425 | 0.462 | 0.276 | 0.460 | 0.706 | 0.313 | 0.695 | 0.883 |
| 27 | EOGHorizontalSignal | 0.798 | 0.781 | 0.787 | 0.798 | 0.814 | 0.798 | 0.796 | 0.626 | 0.313 | 0.827 | 0.849 |
| 28 | EOGVerticalSignal | 0.881 | 0.881 | 0.882 | 0.878 | 0.864 | 0.775 | 0.876 | 0.885 | 0.773 | 0.883 | 0.664 |
| 29 | EthanolLevel | 0.712 | 0.674 | 0.708 | 0.665 | 0.263 | 0.249 | 0.709 | 0.623 | 0.274 | 0.713 | 0.753 |
| 30 | FaceAll | 0.983 | 0.985 | 0.984 | 0.974 | 0.899 | 0.559 | 0.984 | 0.987 | 0.940 | 0.988 | 0.989 |
| 31 | FacesUCR | 0.987 | 0.978 | 0.978 | 0.973 | 0.942 | 0.550 | 0.978 | 0.990 | 0.920 | 0.986 | 0.989 |
| 32 | Fish | 0.923 | 0.919 | 0.917 | 0.880 | 0.477 | 0.143 | 0.943 | 0.960 | 0.340 | 0.951 | 0.923 |
| 33 | FordA | 0.928 | 0.927 | 0.928 | 0.922 | 0.918 | 0.898 | 0.936 | 0.942 | 0.767 | 0.927 | 0.949 |
| 34 | FordB | 0.903 | 0.900 | 0.898 | 0.895 | 0.887 | 0.878 | 0.900 | 0.917 | 0.751 | 0.905 | 0.934 |
| 35 | FreezerRegularTrain | 0.998 | 0.999 | 0.999 | 0.997 | 0.774 | 0.763 | 0.992 | 0.998 | 0.500 | 0.999 | 1.000 |
| 36 | FreezerSmallTrain | 0.992 | 0.998 | 0.998 | 0.998 | 0.710 | 0.762 | 0.998 | 0.999 | 0.501 | 0.999 | 1.000 |
| 37 | GesturePebbleZ1 | 0.865 | 0.875 | 0.866 | 0.869 | 0.816 | 0.420 | 0.875 | 0.891 | 0.888 | 0.885 | 0.957 |
| 38 | GesturePebbleZ2 | 0.872 | 0.905 | 0.878 | 0.852 | 0.844 | 0.475 | 0.876 | 0.911 | 0.915 | 0.908 | 0.954 |
| 39 | GunPoint | 0.995 | 1.000 | 1.000 | 0.990 | 0.940 | 0.775 | 1.000 | 0.990 | 0.900 | 1.000 | 0.998 |
| 40 | GunPointAgeSpan | 0.836 | 0.985 | 0.985 | 0.989 | 0.919 | 0.978 | 0.992 | 0.996 | 0.907 | 0.993 | 0.997 |
| 41 | GunPointMaleVersusFemale | 0.998 | 0.996 | 0.998 | 0.996 | 0.989 | 0.980 | 1.000 | 1.000 | 0.900 | 1.000 | 1.000 |
| 42 | GunPointOldVersusYoung | 0.972 | 0.927 | 0.907 | 0.922 | 0.842 | 0.758 | 0.983 | 0.993 | 0.628 | 0.987 | 0.989 |
| 43 | Ham | 0.678 | 0.701 | 0.794 | 0.743 | 0.678 | 0.519 | 0.682 | 0.776 | 0.730 | 0.725 | 0.855 |
| 44 | HandOutlines | 0.887 | 0.892 | 0.892 | 0.876 | 0.713 | 0.639 | 0.875 | 0.866 | 0.701 | 0.931 | 0.907 |
| 45 | Haptics | 0.467 | 0.465 | 0.475 | 0.437 | 0.322 | 0.214 | 0.504 | 0.460 | 0.337 | 0.531 | 0.560 |
| 46 | Herring | 0.540 | 0.650 | 0.656 | 0.625 | 0.563 | 0.602 | 0.691 | 0.624 | 0.562 | 0.587 | 0.705 |
| 47 | HouseTwenty | 0.956 | 0.994 | 0.994 | 0.994 | 0.956 | 0.906 | 0.988 | 0.969 | 0.944 | 0.963 | 0.948 |
| 48 | InlineSkate | 0.462 | 0.565 | 0.557 | 0.518 | 0.389 | 0.168 | 0.526 | 0.448 | 0.223 | 0.705 | 0.560 |
| 49 | InsectEPGRegularTrain | 0.974 | 0.994 | 0.994 | 0.997 | 0.997 | 0.961 | 0.990 | 0.997 | 0.974 | 0.987 | 0.981 |
| 50 | InsectEPGSmallTrain | 0.974 | 0.970 | 0.974 | 0.959 | 0.966 | 0.778 | 0.993 | 0.989 | 0.955 | 0.996 | 0.971 |
| 51 | InsectWingbeatSound | 0.546 | 0.544 | 0.491 | 0.439 | 0.355 | 0.272 | 0.574 | 0.523 | 0.271 | 0.746 | 0.717 |
| 52 | ItalyPowerDemand | 0.972 | 0.973 | 0.975 | 0.976 | 0.789 | 0.958 | 0.974 | 0.981 | 0.838 | 0.979 | 0.982 |
| 53 | LargeKitchenAppliances | 0.919 | 0.936 | 0.939 | 0.919 | 0.937 | 0.624 | 0.931 | 0.939 | 0.843 | 0.953 | 0.908 |
| 54 | Lightning2 | 0.794 | 0.726 | 0.605 | 0.713 | 0.636 | 0.661 | 0.754 | 0.811 | 0.629 | 0.835 | 0.810 |
| 55 | Mallat | 0.991 | 0.990 | 0.992 | 0.990 | 0.340 | 0.321 | 0.993 | 0.991 | 0.579 | 0.995 | 0.992 |
| 56 | Meat | 0.967 | 0.658 | 0.975 | 0.858 | 0.617 | 0.333 | 0.965 | 0.908 | 0.333 | 0.975 | 0.992 |
| 57 | MedicalImages | 0.763 | 0.777 | 0.787 | 0.753 | 0.589 | 0.521 | 0.790 | 0.778 | 0.521 | 0.798 | 0.802 |
| 58 | MelbournePedestrian | 0.912 | 0.903 | 0.904 | 0.903 | 0.564 | 0.738 | 0.921 | 0.929 | 0.486 | 0.921 | 0.928 |
| 59 | MiddlePhalanxOutlineAgeGroup | 0.742 | 0.753 | 0.740 | 0.758 | 0.671 | 0.729 | 0.746 | 0.769 | 0.722 | 0.798 | 0.778 |
| 60 | MiddlePhalanxOutlineCorrect | 0.837 | 0.798 | 0.804 | 0.721 | 0.682 | 0.622 | 0.845 | 0.856 | 0.626 | 0.853 | 0.859 |
| 61 | MiddlePhalanxTW | 0.609 | 0.615 | 0.626 | 0.612 | 0.584 | 0.597 | 0.621 | 0.659 | 0.597 | 0.657 | 0.662 |

| | | | | | | | | | | | | |
|-----------|--------------------------------|--------------|--------------|--------------|--------------|--------------|----------|--------------|--------------|--------------|--------------|--------------|
| 62 | MixedShapesRegularTrain | 0.969 | 0.968 | 0.962 | 0.966 | 0.744 | 0.683 | 0.972 | 0.977 | 0.378 | 0.974 | 0.978 |
| 63 | MixedShapesSmallTrain | 0.962 | 0.966 | 0.969 | 0.955 | 0.587 | 0.742 | 0.972 | 0.972 | 0.436 | 0.977 | 0.968 |
| 64 | MoteStrain | 0.969 | 0.973 | 0.971 | 0.969 | 0.967 | 0.943 | 0.970 | 0.976 | 0.977 | 0.970 | 0.975 |
| 65 | NonInvasiveFetalECGThorax1 | 0.299 | 0.395 | 0.403 | 0.081 | 0.109 | 0.052 | 0.491 | 0.300 | 0.092 | 0.444 | 0.894 |
| 66 | NonInvasiveFetalECGThorax2 | 0.351 | 0.440 | 0.460 | 0.179 | 0.109 | 0.048 | 0.632 | 0.396 | 0.082 | 0.520 | 0.926 |
| 67 | OSULeaf | 0.973 | 0.959 | 0.955 | 0.881 | 0.880 | 0.479 | 0.975 | 0.982 | 0.668 | 0.982 | 0.897 |
| 68 | PhalangesOutlinesCorrect | 0.420 | 0.445 | 0.457 | 0.437 | 0.330 | 0.219 | 0.443 | 0.384 | 0.254 | 0.477 | 0.459 |
| 69 | Phoneme | 0.852 | 0.858 | 0.846 | 0.847 | 0.661 | 0.640 | 0.873 | 0.860 | 0.685 | 0.853 | 0.865 |
| 70 | PLAID | 0.367 | 0.407 | 0.405 | 0.398 | 0.449 | 0.212 | 0.435 | 0.395 | 0.372 | 0.396 | 0.402 |
| 71 | Plane | 1.000 | 1.000 | 1.000 | 1.000 | 0.914 | 0.514 | 1.000 | 1.000 | 0.538 | 1.000 | 1.000 |
| 72 | PowerCons | 0.867 | 0.881 | 0.869 | 0.856 | 0.853 | 0.800 | 0.908 | 0.894 | 0.850 | 0.889 | 0.950 |
| 73 | ProximalPhalanxOutlineAgeGroup | 0.850 | 0.843 | 0.840 | 0.841 | 0.700 | 0.787 | 0.845 | 0.843 | 0.734 | 0.865 | 0.870 |
| 74 | ProximalPhalanxOutlineCorrect | 0.887 | 0.877 | 0.897 | 0.884 | 0.668 | 0.690 | 0.894 | 0.907 | 0.801 | 0.873 | 0.878 |
| 75 | ProximalPhalanxTW | 0.759 | 0.804 | 0.807 | 0.804 | 0.640 | 0.728 | 0.814 | 0.805 | 0.516 | 0.840 | 0.813 |
| 76 | RefrigerationDevices | 0.603 | 0.689 | 0.720 | 0.693 | 0.731 | 0.544 | 0.700 | 0.600 | 0.627 | 0.779 | 0.637 |
| 77 | ScreenType | 0.693 | 0.717 | 0.724 | 0.720 | 0.625 | 0.431 | 0.687 | 0.687 | 0.659 | 0.720 | 0.627 |
| 78 | SemgHandGenderCh2 | 0.891 | 0.848 | 0.853 | 0.859 | 0.792 | 0.678 | 0.890 | 0.903 | 0.783 | 0.912 | 0.872 |
| 79 | SemgHandMovementCh2 | 0.623 | 0.586 | 0.600 | 0.548 | 0.409 | 0.271 | 0.614 | 0.630 | 0.444 | 0.662 | 0.657 |
| 80 | SemgHandSubjectCh2 | 0.828 | 0.798 | 0.799 | 0.732 | 0.582 | 0.537 | 0.846 | 0.861 | 0.700 | 0.858 | 0.892 |
| 81 | ShapeletSim | 0.995 | 0.985 | 0.995 | 0.995 | 0.975 | 0.800 | 0.990 | 1.000 | 0.995 | 1.000 | 0.989 |
| 82 | SmallKitchenAppliances | 0.779 | 0.797 | 0.789 | 0.800 | 0.728 | 0.589 | 0.805 | 0.801 | 0.753 | 0.827 | 0.767 |
| 83 | SmoothSubspace | 0.967 | 0.960 | 0.967 | 0.957 | 0.723 | 0.913 | 0.977 | 0.967 | 0.835 | 0.970 | 0.967 |
| 84 | SonyAIBORobotSurface1 | 0.995 | 0.997 | 0.995 | 0.995 | 0.998 | 0.978 | 0.998 | 0.995 | 0.982 | 0.998 | 0.999 |
| 85 | SonyAIBORobotSurface2 | 0.998 | 0.994 | 0.995 | 0.995 | 0.992 | 0.981 | 0.989 | 0.997 | 0.980 | 0.996 | 0.998 |
| 86 | StarLightCurves | 0.978 | 0.979 | 0.978 | 0.979 | 0.979 | 0.850 | 0.977 | 0.980 | 0.935 | 0.979 | 0.981 |
| 87 | Strawberry | 0.963 | 0.959 | 0.954 | 0.954 | 0.686 | 0.700 | 0.967 | 0.970 | 0.654 | 0.977 | 0.980 |
| 88 | SwedishLeaf | 0.968 | 0.956 | 0.948 | 0.941 | 0.814 | 0.553 | 0.953 | 0.978 | 0.473 | 0.979 | 0.926 |
| 89 | Symbols | 0.995 | 0.994 | 0.996 | 0.935 | 0.830 | 0.929 | 0.994 | 0.998 | 0.749 | 0.992 | 0.995 |
| 90 | SyntheticControl | 0.987 | 0.995 | 0.990 | 0.992 | 0.987 | 0.988 | 0.985 | 0.992 | 0.978 | 0.988 | 0.995 |
| 91 | ToeSegmentation1 | 0.971 | 0.951 | 0.940 | 0.952 | 0.978 | 0.951 | 0.974 | 0.978 | 0.914 | 0.978 | 0.952 |
| 92 | ToeSegmentation2 | 0.910 | 0.885 | 0.855 | 0.861 | 0.880 | 0.807 | 0.921 | 0.940 | 0.923 | 0.922 | 0.940 |
| 93 | Trace | 1.000 | 1.000 | 1.000 | 1.000 | 0.990 | 0.635 | 1.000 | 1.000 | 0.920 | 1.000 | 1.000 |
| 94 | TwoLeadECG | 1.000 | 1.000 | 1.000 | 1.000 | 1.000 | 0.995 | 1.000 | 1.000 | 0.990 | 1.000 | 1.000 |
| 95 | TwoPatterns | 0.905 | 0.906 | 0.901 | 0.909 | 0.886 | 0.833 | 0.915 | 0.918 | 0.903 | 0.918 | 1.000 |
| 96 | UMD | 0.983 | 0.983 | 0.983 | 0.972 | 0.911 | 0.750 | 0.978 | 0.996 | 0.833 | 0.994 | 0.999 |
| 97 | UWaveGestureLibraryAll | 0.874 | 0.880 | 0.874 | 0.860 | 0.668 | 0.478 | 0.879 | 0.876 | 0.535 | 0.923 | 0.977 |
| 98 | UWaveGestureLibraryX | 0.806 | 0.760 | 0.769 | 0.745 | 0.437 | 0.564 | 0.793 | 0.809 | 0.698 | 0.795 | 0.863 |
| 99 | UWaveGestureLibraryY | 0.707 | 0.721 | 0.722 | 0.657 | 0.530 | 0.503 | 0.729 | 0.726 | 0.626 | 0.717 | 0.808 |
| 100 | UWaveGestureLibraryZ | 0.788 | 0.784 | 0.781 | 0.765 | 0.480 | 0.534 | 0.784 | 0.800 | 0.631 | 0.794 | 0.812 |
| 101 | Wafer | 0.999 | 0.999 | 0.999 | 0.999 | 0.913 | 0.894 | 0.999 | 1.000 | 0.935 | 1.000 | 1.000 |
| 102 | Wine | 0.892 | 0.797 | 0.813 | 0.783 | 0.514 | 0.495 | 0.788 | 0.801 | 0.550 | 0.829 | 0.892 |
| 103 | WordSynonyms | 0.467 | 0.465 | 0.427 | 0.387 | 0.401 | 0.223 | 0.487 | 0.434 | 0.244 | 0.505 | 0.792 |
| 104 | Worms | 0.721 | 0.632 | 0.636 | 0.648 | 0.675 | 0.508 | 0.750 | 0.721 | 0.504 | 0.658 | 0.597 |
| 105 | WormsTwoClass | 0.760 | 0.761 | 0.768 | 0.760 | 0.756 | 0.670 | 0.783 | 0.771 | 0.562 | 0.728 | 0.802 |
| 106 | Yoga | 0.906 | 0.923 | 0.924 | 0.928 | 0.792 | 0.596 | 0.935 | 0.939 | 0.735 | 0.947 | 0.946 |
| Avg. Rank | | 5.50 | 5.21 | 5.20 | 6.33 | 8.71 | 10.29 | 4.36 | 3.73 | 9.27 | 2.88 | 2.63 |
| Win | | 7 | 7 | 6 | 5 | 4 | 0 | 11 | 18 | 2 | 28 | 64 |
| P-value | | 1.44E-05 | 6.31E-06 | 1.59E-05 | 4.20E-06 | 1.52E-16 | 3.29E-24 | 1.84E-04 | 3.46E-04 | 9.40E-20 | 2.19E-02 | - |

Table 4: The detailed test classification accuracy comparisons on 106 UCR time series datasets with a 40% labeling ratio. Win denotes the number of datasets in which the corresponding baseline achieved the best test accuracy. The best is in **bold**.

| ID | Dataset | ST | LTS | FFS | ADSN | DiffShape |
|------------------|-----------------------|----------|----------|----------|----------|--------------|
| 1 | ChlorineConcentration | 0.510 | 0.445 | 0.536 | 0.232 | 0.749 |
| 2 | DiatomSizeReduction | 0.776 | 0.351 | 0.636 | 0.105 | 0.985 |
| 3 | ECGFiveDays | 0.925 | 0.727 | 0.778 | 0.916 | 1.000 |
| 4 | GunPoint | 0.725 | 0.720 | 0.694 | 0.760 | 0.930 |
| 5 | ItalyPowerDemand | 0.876 | 0.907 | 0.832 | 0.938 | 0.972 |
| 6 | MedicalImages | 0.507 | 0.521 | 0.521 | 0.520 | 0.637 |
| 7 | MoteStrain | 0.858 | 0.789 | 0.728 | 0.718 | 0.921 |
| 8 | SonyAIBORobotSurface1 | 0.961 | 0.936 | 0.842 | 0.929 | 0.987 |
| 9 | Symbols | 0.613 | 0.463 | 0.433 | 0.549 | 0.981 |
| 10 | SyntheticControl | 0.558 | 0.695 | 0.475 | 0.523 | 0.995 |
| 11 | Trace | 0.320 | 0.350 | 0.500 | 0.455 | 1.000 |
| 12 | TwoLeadECG | 0.973 | 0.870 | 0.775 | 0.962 | 1.000 |
| Avg. Rank | | 2.92 | 3.50 | 3.92 | 3.58 | 1.00 |
| Win | | 0 | 0 | 0 | 0 | 12 |
| P-value | | 1.60E-03 | 3.78E-04 | 2.86E-05 | 1.44E-03 | - |

Table 5: The detailed test classification accuracy comparisons on 12 UCR time series datasets with a 10% labeling ratio.

| ID | Dataset | ST | LTS | FFS | ADSN | DiffShape |
|------------------|-----------------------|----------|----------|----------|----------|--------------|
| 1 | ChlorineConcentration | 0.520 | 0.441 | 0.538 | 0.232 | 0.898 |
| 2 | DiatomSizeReduction | 0.752 | 0.416 | 0.646 | 0.106 | 0.991 |
| 3 | ECGFiveDays | 0.897 | 0.901 | 0.959 | 0.993 | 1.000 |
| 4 | GunPoint | 0.790 | 0.725 | 0.750 | 0.660 | 0.992 |
| 5 | ItalyPowerDemand | 0.901 | 0.932 | 0.818 | 0.938 | 0.975 |
| 6 | MedicalImages | 0.460 | 0.526 | 0.524 | 0.501 | 0.701 |
| 7 | MoteStrain | 0.899 | 0.832 | 0.839 | 0.883 | 0.959 |
| 8 | SonyAIBORobotSurface1 | 0.966 | 0.939 | 0.824 | 0.916 | 0.991 |
| 9 | Symbols | 0.455 | 0.845 | 0.350 | 0.751 | 0.991 |
| 10 | SyntheticControl | 0.513 | 0.617 | 0.555 | 0.740 | 0.995 |
| 11 | Trace | 0.535 | 0.405 | 0.325 | 0.690 | 1.000 |
| 12 | TwoLeadECG | 0.983 | 0.945 | 0.829 | 0.971 | 1.000 |
| Avg. Rank | | 3.25 | 3.50 | 3.92 | 3.33 | 1.00 |
| Win | | 0 | 0 | 0 | 0 | 12 |
| P-value | | 6.08E-04 | 7.37E-04 | 1.95E-04 | 3.37E-03 | - |

Table 6: The detailed test classification accuracy comparisons on 12 UCR time series datasets with a 20% labeling ratio.

| ID | Dataset | ST | LTS | FFS | ADSN | DiffShape |
|------------------|-----------------------|----------|----------|----------|----------|--------------|
| 1 | ChlorineConcentration | 0.625 | 0.462 | 0.541 | 0.232 | 0.978 |
| 2 | DiatomSizeReduction | 0.795 | 0.512 | 0.533 | 0.106 | 0.999 |
| 3 | ECGFiveDays | 0.991 | 0.940 | 0.998 | 0.921 | 1.000 |
| 4 | GunPoint | 0.880 | 0.810 | 0.690 | 0.905 | 0.998 |
| 5 | ItalyPowerDemand | 0.912 | 0.937 | 0.952 | 0.935 | 0.982 |
| 6 | MedicalImages | 0.511 | 0.522 | 0.530 | 0.528 | 0.802 |
| 7 | MoteStrain | 0.885 | 0.866 | 0.861 | 0.921 | 0.975 |
| 8 | SonyAIBORobotSurface1 | 0.976 | 0.957 | 0.745 | 0.961 | 0.999 |
| 9 | Symbols | 0.629 | 0.444 | 0.573 | 0.645 | 0.995 |
| 10 | SyntheticControl | 0.495 | 0.753 | 0.575 | 0.620 | 0.995 |
| 11 | Trace | 0.580 | 0.550 | 0.569 | 0.735 | 1.000 |
| 12 | TwoLeadECG | 0.985 | 0.978 | 0.969 | 0.987 | 1.000 |
| Avg. Rank | | 3.25 | 3.92 | 3.67 | 3.17 | 1.00 |
| Win | | 0 | 0 | 0 | 0 | 12 |
| P-value | | 9.24E-04 | 6.86E-04 | 1.56E-04 | 4.02E-03 | - |

Table 7: The detailed test classification accuracy comparisons on 12 UCR time series datasets with a 40% labeling ratio.

| ID | Dataset | Supervised | LTS | ADSN | SemiTime | SSSTC | MTFC | TS-TFC | DiffShape |
|------------------|-----------------------|------------|----------|----------|----------|----------|----------|--------------|--------------|
| 1 | ChlorineConcentration | 0.470 | 0.234 | 0.000 | 0.507 | 0.509 | 0.376 | 0.500 | 0.516 |
| 2 | DiatomSizeReduction | 0.879 | 0.304 | 0.000 | 0.832 | 0.838 | 0.709 | 0.873 | 0.966 |
| 3 | ECGFiveDays | 0.748 | 0.522 | 0.584 | 0.751 | 0.758 | 0.750 | 0.810 | 0.975 |
| 4 | GunPoint | 0.575 | 0.500 | 0.565 | 0.665 | 0.605 | 0.550 | 0.580 | 0.745 |
| 5 | ItalyPowerDemand | 0.845 | 0.501 | 0.791 | 0.874 | 0.882 | 0.834 | 0.875 | 0.955 |
| 6 | MedicalImages | 0.446 | 0.085 | 0.217 | 0.416 | 0.422 | 0.292 | 0.378 | 0.464 |
| 7 | MoteStrain | 0.853 | 0.462 | 0.660 | 0.858 | 0.859 | 0.866 | 0.874 | 0.868 |
| 8 | SonyAIBORobotSurface1 | 0.919 | 0.438 | 0.704 | 0.944 | 0.936 | 0.870 | 0.950 | 0.879 |
| 9 | Symbols | 0.946 | 0.137 | 0.222 | 0.956 | 0.961 | 0.620 | 0.962 | 0.962 |
| 10 | SyntheticControl | 0.887 | 0.168 | 0.295 | 0.943 | 0.938 | 0.868 | 0.880 | 0.967 |
| 11 | Trace | 0.960 | 0.350 | 0.275 | 0.945 | 0.955 | 0.565 | 0.945 | 0.970 |
| 12 | TwoLeadECG | 0.871 | 0.508 | 0.547 | 0.919 | 0.927 | 0.501 | 0.886 | 0.930 |
| Avg. Rank | | 4.25 | 7.67 | 7.08 | 3.50 | 2.92 | 5.92 | 3.08 | 1.42 |
| Win | | 0 | 0 | 0 | 0 | 0 | 0 | 3 | 10 |
| P-value | | 5.28E-03 | 8.07E-07 | 6.81E-05 | 2.14E-02 | 2.08E-02 | 2.18E-04 | 8.01E-03 | - |

Table 8: The detailed test classification accuracy comparisons on 12 UCR time series datasets with 2 label samples per class.

| ID | Dataset | Supervised | LTS | ADSN | SemiTime | SSSTC | MTFC | TS-TFC | DiffShape |
|------------------|-----------------------|------------|----------|----------|----------|----------|----------|--------------|--------------|
| 1 | ChlorineConcentration | 0.491 | 0.232 | 0.000 | 0.522 | 0.527 | 0.478 | 0.474 | 0.536 |
| 2 | DiatomSizeReduction | 0.981 | 0.304 | 0.000 | 0.969 | 0.978 | 0.608 | 0.985 | 0.988 |
| 3 | ECGFiveDays | 0.852 | 0.500 | 0.655 | 0.843 | 0.866 | 0.791 | 0.941 | 0.994 |
| 4 | GunPoint | 0.885 | 0.500 | 0.665 | 0.935 | 0.865 | 0.635 | 0.910 | 0.950 |
| 5 | ItalyPowerDemand | 0.910 | 0.501 | 0.792 | 0.942 | 0.931 | 0.854 | 0.922 | 0.966 |
| 6 | MedicalImages | 0.546 | 0.073 | 0.318 | 0.590 | 0.564 | 0.440 | 0.587 | 0.596 |
| 7 | MoteStrain | 0.862 | 0.462 | 0.622 | 0.868 | 0.874 | 0.872 | 0.887 | 0.882 |
| 8 | SonyAIBORobotSurface1 | 0.952 | 0.438 | 0.578 | 0.952 | 0.952 | 0.886 | 0.961 | 0.931 |
| 9 | Symbols | 0.956 | 0.178 | 0.323 | 0.961 | 0.961 | 0.600 | 0.978 | 0.960 |
| 10 | SyntheticControl | 0.957 | 0.187 | 0.263 | 0.963 | 0.967 | 0.862 | 0.958 | 0.990 |
| 11 | Trace | 0.960 | 0.110 | 0.355 | 0.985 | 0.990 | 0.975 | 0.995 | 1.000 |
| 12 | TwoLeadECG | 0.950 | 0.471 | 0.548 | 0.966 | 0.972 | 0.501 | 0.978 | 0.985 |
| Avg. Rank | | 4.50 | 7.83 | 7.00 | 3.25 | 3.00 | 5.83 | 2.58 | 1.67 |
| Win | | 0 | 0 | 0 | 0 | 0 | 0 | 3 | 9 |
| P-value | | 3.07E-03 | 1.37E-07 | 1.44E-05 | 3.96E-02 | 1.97E-02 | 8.12E-04 | 3.38E-02 | - |

Table 9: The detailed test classification accuracy comparisons on 12 UCR time series datasets with 5 label samples per class.

| ID | Dataset | Supervised | LTS | ADSN | SemiTime | SSSTC | MTFC | TS-TFC | DiffShape |
|------------------|-----------------------|------------|----------|----------|--------------|--------------|--------------|--------------|--------------|
| 1 | ChlorineConcentration | 0.512 | 0.235 | 0.000 | 0.533 | 0.537 | 0.544 | 0.509 | 0.542 |
| 2 | DiatomSizeReduction | 0.982 | 0.304 | 0.000 | 0.988 | 0.988 | 0.528 | 0.985 | 0.991 |
| 3 | ECGFiveDays | 0.973 | 0.499 | 0.647 | 0.951 | 0.930 | 0.867 | 0.988 | 0.999 |
| 4 | GunPoint | 0.950 | 0.500 | 0.650 | 0.975 | 0.955 | 0.605 | 0.979 | 0.980 |
| 5 | ItalyPowerDemand | 0.954 | 0.501 | 0.553 | 0.965 | 0.956 | 0.935 | 0.957 | 0.971 |
| 6 | MedicalImages | 0.627 | 0.065 | 0.337 | 0.632 | 0.637 | 0.366 | 0.627 | 0.639 |
| 7 | MoteStrain | 0.880 | 0.462 | 0.596 | 0.889 | 0.896 | 0.893 | 0.892 | 0.892 |
| 8 | SonyAIBORobotSurface1 | 0.968 | 0.438 | 0.752 | 0.977 | 0.973 | 0.921 | 0.979 | 0.974 |
| 9 | Symbols | 0.966 | 0.132 | 0.306 | 0.969 | 0.971 | 0.809 | 0.978 | 0.968 |
| 10 | SyntheticControl | 0.983 | 0.220 | 0.297 | 0.975 | 0.982 | 0.917 | 0.980 | 0.993 |
| 11 | Trace | 0.980 | 0.080 | 0.450 | 1.000 | 1.000 | 0.960 | 1.000 | 1.000 |
| 12 | TwoLeadECG | 0.969 | 0.500 | 0.565 | 0.976 | 0.983 | 0.682 | 0.990 | 0.993 |
| Avg. Rank | | 4.58 | 7.83 | 7.08 | 3.17 | 2.83 | 5.33 | 2.75 | 1.75 |
| Win | | 0 | 0 | 0 | 1 | 2 | 1 | 3 | 8 |
| P-value | | 3.95E-05 | 1.28E-07 | 5.09E-06 | 1.94E-02 | 3.93E-02 | 2.51E-03 | 3.56E-02 | - |

Table 10: The detailed test classification accuracy comparisons on 12 UCR time series datasets with 10 label samples per class.

| ID | Dataset | DiffShape | w/o Diff | real subsequence | random shape | w/o Language | w/o Diff & Language |
|------------------|-----------------------|--------------|--------------|------------------|--------------|--------------|---------------------|
| 1 | ChlorineConcentration | 0.749 | 0.614 | 0.613 | 0.577 | 0.581 | 0.571 |
| 2 | DiatomSizeReduction | 0.985 | 0.971 | 0.972 | 0.963 | 0.960 | 0.955 |
| 3 | ECGFiveDays | 1.000 | 1.000 | 1.000 | 1.000 | 1.000 | 0.981 |
| 4 | GunPoint | 0.930 | 0.920 | 0.920 | 0.925 | 0.925 | 0.915 |
| 5 | ItalyPowerDemand | 0.972 | 0.966 | 0.969 | 0.961 | 0.953 | 0.947 |
| 6 | MedicalImages | 0.637 | 0.615 | 0.618 | 0.616 | 0.589 | 0.543 |
| 7 | MoteStrain | 0.921 | 0.917 | 0.910 | 0.914 | 0.921 | 0.913 |
| 8 | SonyAIBORobotSurface1 | 0.987 | 0.972 | 0.979 | 0.978 | 0.963 | 0.962 |
| 9 | Symbols | 0.981 | 0.979 | 0.978 | 0.971 | 0.977 | 0.961 |
| 10 | SyntheticControl | 0.995 | 0.992 | 0.992 | 0.992 | 0.992 | 0.992 |
| 11 | Trace | 1.000 | 0.950 | 0.970 | 0.953 | 0.975 | 0.975 |
| 12 | TwoLeadECG | 1.000 | 0.993 | 0.994 | 0.992 | 0.989 | 0.991 |
| Avg. Rank | | 1.00 | 3.08 | 2.75 | 3.50 | 3.58 | 5.17 |
| Win | | 12 | 1 | 1 | 1 | 1 | 0 |
| P-value | | - | 3.35E-02 | 4.39E-02 | 4.14E-02 | 3.04E-02 | 1.22E-02 |

Table 11: The detailed test classification accuracy of ablation study on 12 UCR time series datasets with a 10% labeling ratio.

| Method | | Dataset | |
|--------------------------|--------------------------------|--------------|-----------------------|
| | | Trace | ChlorineConcentration |
| SSL baselines | Supervised (Cross entropy) | 16.22 | 161.15 |
| | Pseudo-Label (Lee et al. 2013) | 26.35 | 902.30 |
| | MTL (Jawed et al. 2020) | 167.50 | 2671.55 |
| | SemiTime (Fan et al. 2021) | 898.40 | 3263.68 |
| | SSSTC (Xi et al. 2022) | 1030.06 | 4872.84 |
| | MTFC (Wei et al. 2023) | 217.27 | 4325.12 |
| | TS-TFC (Liu et al. 2023) | 30.19 | 986.95 |
| Shapelet-based baselines | ST (Lines et al. 2012) | 21487.61 | 11190.28 |
| | LTS (Grabocka et al. 2014) | 772.95 | 7343.92 |
| | FSS (Ji et al. 2019), | 129.70 | 4532.16 |
| | ADSN (Ma et al. 2020) | 1991.99 | 42826.91 |
| DiffShape (Ours) | | 92.16 | 2355.10 |

Table 12: Analysis of runtime (in seconds) on the *Trace* and *ChlorineConcentration* time series datasets with a 10% labeling ratio for semi-supervised classification. The best is in **bold**, and the second best is in underlined.

References

- Dau, H. A.; Bagnall, A.; Kamgar, K.; Yeh, C.-C. M.; Zhu, Y.; Gharghabi, S.; Ratanamahatana, C. A.; and Keogh, E. 2019. The UCR time series archive. *IEEE/CAA Journal of Automatica Sinica*, 6(6): 1293–1305.
- Demšar, J. 2006. Statistical comparisons of classifiers over multiple data sets. *The Journal of Machine learning research*, 7: 1–30.
- Eldele, E.; Ragab, M.; Chen, Z.; Wu, M.; Kwok, C. K.; Li, X.; and Guan, C. 2021. Time-series representation learning via temporal and contextual contrasting. *arXiv preprint arXiv:2106.14112*.
- Fan, H.; Zhang, F.; Wang, R.; Huang, X.; and Li, Z. 2021. Semi-supervised time series classification by temporal relation prediction. In *ICASSP 2021-2021 IEEE International Conference on Acoustics, Speech and Signal Processing (ICASSP)*, 3545–3549. IEEE.
- Grabocka, J.; Schilling, N.; Wistuba, M.; and Schmidt-Thieme, L. 2014. Learning time-series shapelets. In *Proceedings of the 20th ACM SIGKDD international conference on Knowledge discovery and data mining*, 392–401.
- Isen, A.; Tolias, G.; Avrithis, Y.; and Chum, O. 2019. Label propagation for deep semi-supervised learning. In *Proceedings of the IEEE/CVF conference on computer vision and pattern recognition*, 5070–5079.
- Ismail Fawaz, H.; Forestier, G.; Weber, J.; Idoumghar, L.; and Muller, P.-A. 2019. Deep learning for time series classification: a review. *Data mining and knowledge discovery*, 33(4): 917–963.
- Jawed, S.; Grabocka, J.; and Schmidt-Thieme, L. 2020. Self-supervised learning for semi-supervised time series classification. In *Advances in Knowledge Discovery and Data Mining: 24th Pacific-Asia Conference, PAKDD 2020, Singapore, May 11–14, 2020, Proceedings, Part I 24*, 499–511. Springer.
- Ji, C.; Zhao, C.; Liu, S.; Yang, C.; Pan, L.; Wu, L.; and Meng, X. 2019. A fast shapelet selection algorithm for time series classification. *Computer networks*, 148: 231–240.
- Laine, S.; and Aila, T. 2016. Temporal ensembling for semi-supervised learning. *arXiv preprint arXiv:1610.02242*.
- Lee, D.-H.; et al. 2013. Pseudo-label: The simple and efficient semi-supervised learning method for deep neural networks. In *Workshop on challenges in representation learning, ICML*, volume 3, 896. Atlanta.
- Lines, J.; Davis, L. M.; Hills, J.; and Bagnall, A. 2012. A shapelet transform for time series classification. In *Proceedings of the 18th ACM SIGKDD international conference on Knowledge discovery and data mining*, 289–297.
- Liu, Z.; Ma, Q.; Ma, P.; and Wang, L. 2023. Temporal-Frequency Co-training for Time Series Semi-supervised Learning. In *Proceedings of the AAAI Conference on Artificial Intelligence*, volume 37, 8923–8931.
- Ma, Q.; Zhuang, W.; Li, S.; Huang, D.; and Cottrell, G. 2020. Adversarial dynamic shapelet networks. In *Proceedings of the AAAI conference on artificial intelligence*, volume 34, 5069–5076.
- Middlehurst, M.; Schäfer, P.; and Bagnall, A. 2023. Bake off redux: a review and experimental evaluation of recent time series classification algorithms. *arXiv preprint arXiv:2304.13029*.
- Van der Maaten, L.; and Hinton, G. 2008. Visualizing data using t-SNE. *Journal of machine learning research*, 9(11).
- Wei, C.; Wang, Z.; Yuan, J.; Li, C.; and Chen, S. 2023. Time-frequency based multi-task learning for semi-supervised time series classification. *Information Sciences*, 619: 762–780.
- Xi, L.; Yun, Z.; Liu, H.; Wang, R.; Huang, X.; and Fan, H. 2022. Semi-supervised time series classification model with self-supervised learning. *Engineering Applications of Artificial Intelligence*, 116: 105331.